Soils and Rocks Volume 30, N. 3 2007

ISSN 1980-9743

Soils and Rocks

Soils and Rocks

An International Journal of Geotechnical and Geoenvironmental Engineering

Volume 30, N. 3
September-December 2007

Soils and Rocks is an International Journal of Geotechnical and Geoenvironmental Engineering published by

ABMS - Brazilian Association for Soil Mechanics and Geotechnical Engineering
Av. Prof. Almeida Prado, 532, IPT/DEC-Prédio 54
05508-901 São Paulo, SP
Brazil

ABGE - Brazilian Association for Engineering Geology and the Environment
Av. Prof. Almeida Prado, 532, IPT/DIGEO- Prédio 59
05508-901 São Paulo, SP
Brazil

SPG – Portuguese Geotechnical Society
LNEC, Avenida do Brasil, 101
1700-066 Lisboa
Portugal

Issue Date: *December 2007*

Issue: *3,200 copies*

Manuscript Submission: *For review criteria and manuscript submission information, see Instructions for Authors at the end.*

SOILS and ROCKS

An International Journal of Geotechnical and Geoenvironmental

Editor Ennio Marques Palmeira - University of Brasília, Brazil

Co-editor Ricardo Oliveira - COBA, Portugal

Soils and Rocks publishes papers in English in the broad fields of Geotechnical Engineering, Engineering Geology and Geo-environmental Engineering. The Journal is published in April, August and December. Subscription price is US$ 90.00 per year. The journal, with the name "Solos e Rochas", was first published in 1978 by the Graduate School of Engineering-Federal University of Rio de Janeiro (COPPE-UFRJ). In 1980 it became the official magazine of the Brazilian Association for Soil Mechanics and Geotechnical Engineering (ABMS), acquiring the national character that had been the intention of its founders. In 1986 it also became the official Journal of the Brazilian Association for Engineering Geology and the Environment (ABGE) and in 1999 became the Latin American Geotechnical Journal, following the support of Latin-American representatives gathered for the Pan-American Conference of Guadalajara (1996). In 2007 the journal acquired the status of an international journal under the name of Soils and Rocks, published by the Brazilian Association for Soil Mechanics and Geotechnical Engineering (ABMS), Brazilian Association for Engineering Geology and the Environment (ABGE) and Portuguese Geotechnical Society (SPG).

Soils and Rocks

1978,	1 (1, 2)
1979,	1 (3), 2 (1,2)
1980-1983,	3-6 (1, 2, 3)
1984,	7 (single number)
1985-1987,	8-10 (1, 2, 3)
1988-1990,	11-13 (single number)
1991-1992,	14-15 (1, 2)
1993,	16 (1, 2, 3, 4)
1994-2006,	17-29 (1, 2, 3)
2007,	**30(1, 2, 3)**

ISSN 1980-9743 CDU 624.131.1

ISSN 1980-9743

SOILS and ROCKS

An International Journal of Geotechnical and Geoenvironmental

Publication of

ABMS - Brazilian Association for Soil Mechanics and Geotechnical Engineering

ABGE - Brazilian Association for Engineering Geology and the Environment

SPG - Portuguese Geotechnical Society

Volume 30, N. 3, September-December 2007

Table of Contents

Letter from IAEG President

As president of the International Association for Engineering Geology and the Environment (IAEG), I am delighted to support the publication of the new international geo-engineering journal, Soils and Rocks.

The subject matter of the journal is inter-disciplinary. As all good geo-engineering must start with geology, and the journal encompasses both soils and rocks, it will necessarily be relevant to the entire geo-engineering community. The publication of a journal such as Soils and Rocks at this time also coincides with developing trends within the international geo-engineering community for increased collaboration between the geo-engineering disciplines, a trend which I am also committed to supporting. The international nature of this journal is also particularly relevant, as geo-political boundaries are increasingly broken down and the interchange of knowledge around the globe accelerates.

The journal Soils and Rocks represents the long held dream of the Brazilian and Portuguese geotechnical communities and they are to be congratulated on making their dream become a reality. Of course there is more to a journal than pages and papers, a journal is a forum in which ideas and knowledge can be documented, exchanged and ultimately preserved for access by future knowledge seekers. Most importantly, it is an opportunity for individuals to connect and communicate with each other across the globe.

There is absolutely no doubt that there will be an ever increasing demand for geo-engineering knowledge over the next decades. This demand will be created by society's voracious appetite for resources and infrastructure, and by the need for ongoing environmental protection. If we are to meet this demand then journals such as Soils and Rocks will be needed.

I wish you every success in this new venture and look forward to reading what will undoubtedly be a series of prestigious interdisciplinary geo-engineering papers.

With my best regards

Fred Baynes
President IAEG

Articles

Influence of Footing Size and Matric Suction on the Behavior of Shallow Foundations in Collapsible Soil

Ana Paula Fontana Vianna, José Carlos A. Cintra, Nelson Aoki

Abstract. This work analyses the influence of footing size and soil matric suction on the behavior of shallow foundations on unsaturated sandy soil, in terms of bearing capacity and settlements. Fourteen plate load tests were performed at the Experimental Site of USP/São Carlos. Rigid metal plates were used, with diameters varying between 0.20 m and 0.80 m and reinforced concrete footings, with circular base diameter 1.50 m. All the plates and the footings were installed at a depth of 1.5 m. These tests were conducted either with matric suction monitoring using tensiometers installed at the bottom of the hole or with soil flooding. The important role of the matric suction was confirmed. A reduction of the matric suction close to zero causes a great decrease in the bearing capacity and a significant increase in the settlement. In relation to the footing size (B), the bearing capacity as well as the settlements did not present a constant linear increasing variation. This work also proved the importance of considering the soil collapsibility in unsaturated soil shallow foundations design. When this factor is not considered, the calculated allowable bearing capacity may cause very high settlements if soil flooding occurs.

Key words: plate load tests, shallow foundations, footing size, matric suction, bearing capacity, settlements, allowable bearing capacity.

1. Introduction

The footing size has an important effect on the bearing capacity and on the settlements of shallow foundations on sandy soils. In theoretical formulations, as for example Terzaghi's equation (1943) represented by the continuous line in Fig. 1, the bearing capacity (σ_r) varies in a linear and increasing way with the width (B) of the footing.

$$\sigma_r = cN_c S_c + qN_q S_q + \frac{1}{2}\gamma B N_\gamma S_\gamma \quad (1)$$

Nevertheless, such behavior is not valid for footings of small sizes. In this case, contradicting the assumption in theory that σ_r decreases linearly with the decrease of B, the bearing capacity tends to strongly increase with the decrease of the footing width when B is close to zero. The dotted line in Fig. 1 shows this behavior. An evidence of this behavior are the results of CPT tests. The diameter of the cone is only 36 mm but the value of the tip resistance (q_c) is much higher (about 20 a 30 times) than the bearing capacity of foundations of footings installed in the same site and at the same depth.

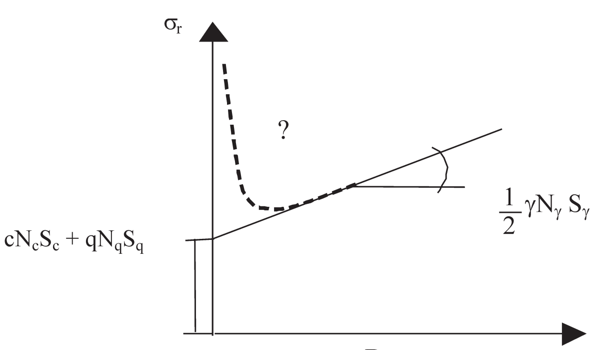

Figure 1 - Bearing capacity in relation to the footing width.

A data analysis performed by De Beer (1965) shows that the bearing capacity factor N_γ increases significantly with the decrease of the footing width for "low" values of B, as shown in Fig. 2.

Similar behaviour is observed in relation to settlements. The theory of linear elasticity shows, for the same stress level, a linear and increasing variation of settlements (ρ) with the foundation size (B) for the case of homogeneous soils (Eq. (2)):

$$\rho = \sigma B\left(\frac{1-\upsilon^2}{E_s}\right) I_\rho \quad (2)$$

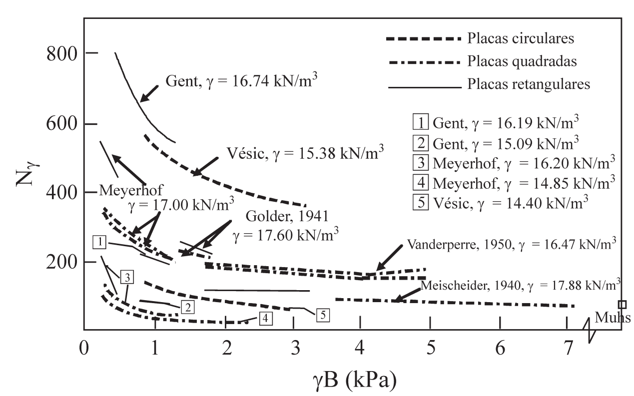

Figure 2 - Effect of the size on the bearing capacity factor N_γ for foundations by footings on sand (De Beer, 1965).

Ana Paula Fontana Vianna, PhD, University of Colorado, Boulder, USA. e-mail: apfvianna@yahoo.com.
José Carlos A. Cintra, Professor, Escola de Engenharia de São Carlos, Universidade de São Paulo, São Carlos, SP, Brazil. e-mail: cintrajc@sc.usp.br.
Nelson Aoki, Professor, Escola de Engenharia de São Carlos, Universidade de São Paulo, São Carlos, SP, Brazil. e-mail: nelson.aoki@uol.com.br.
Submitted on August 18, 2006; Final Acceptance on July 13, 2007; Discussion open until April 30, 2008.

which is represented in Fig. 3 by a straight line towards the origin. Thus, for B tending to zero the settlement also tends to zero.

Gorbunov-Possadov & Davidov (1973) demonstrate the non linear dependence between settlement and the plate sizes and footings, according to Fig. 4. Accordint to these authors: "In the first section AB settlement sharply increases due to the plastic deformations of the soil, whose role decreases with the surface area of the plate, which in fact leads to reduced settlement. Further on, the role of plastic deformations is insignificant, and the dependence of settlement on the plate width becomes linear, which corresponds to the formulas of the theory of elasticity. Tentatively, this section refers to test plate widths from 0.5-0.7 m to 3.0-5.0 m. Then the increase in settlement slows down, and at B > 10 to 20 m settlement becomes practically independent of the plate width."

The matric suction is also another important factor that must be considered in the analysis of foundation behavior on unsaturated soils. This relevant role of the matric suction, in terms of bearing capacity in shallow foundations, was revealed by Fredlund & Rahardjo (1993). They used Terzaghi's bearing capacity equation (1943) and considered the increase of cohesion (c) due to the matric suction (ψ_m):

$$c = c' + \psi_m \operatorname{tg} \phi^b \tag{3}$$

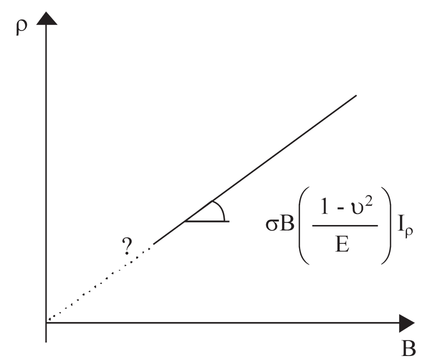

Figure 3 - Settlements of footing in relation to the footing width.

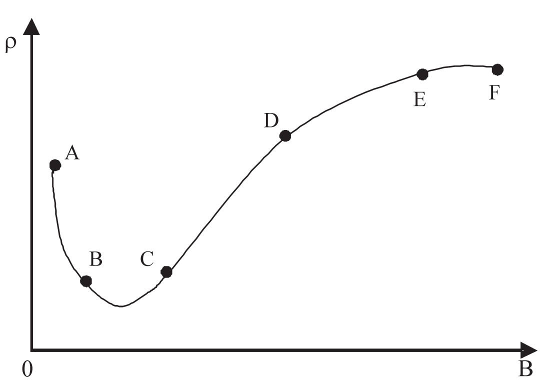

Figure 4 - Settlements variation (ρ) with the size (B) of the footings and rigid plates (Gorbunov-Possadov & Davidov, 1973).

where c' is the effective cohesion and ϕ^b the shearing strength increase rate due to the soil matric suction.

These authors obtained the results shown in Fig. 5 by adopting parameters for the soil (c' = 5 kPa, ϕ' = 20°, ϕ^b = 15° and unit weight γ = 18 kN/m^3) and considering spread footings with B equal to 0.5 and 1.0 m at depth (h) of 0.5 m. A significant increase of the bearing capacity with the matric suction can be observed.

Afterwards, Costa (1999) proved experimentally that in unsaturated soil the matric suction has a great influence on the bearing capacity. Using metal plates load tests with a 0.8 m diameter installed at 1.5 m deep, it was verified that a small increase on the matric suction causes a substantial increase in the bearing capacity. This may be observed in Fig. 6, where ψ_m represents the average matric suction of the soil determined by four tensiometers. Other analyses of this research are shown by Costa *et al.* (2003).

The important role of the matric suction on the behavior of plate-soil system was also found by Macacari (2001) and Cintra *et al.* (2005), for the deeper plates, installed up to 6 m deep.

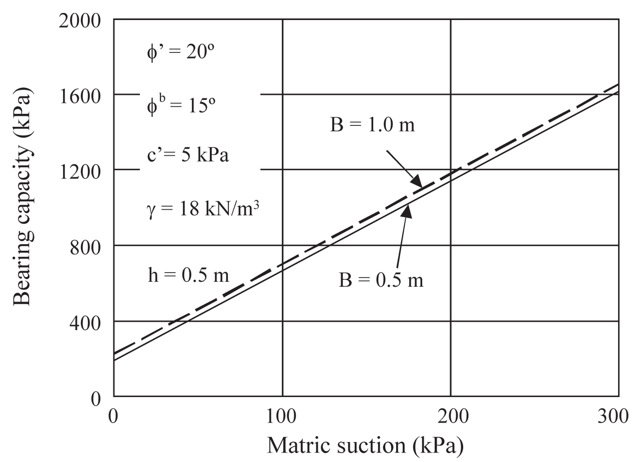

Figure 5 - Bearing capacity of spread footing foundations of width B in relation to the matric suction (Fredlund & Rahardjo, 1993).

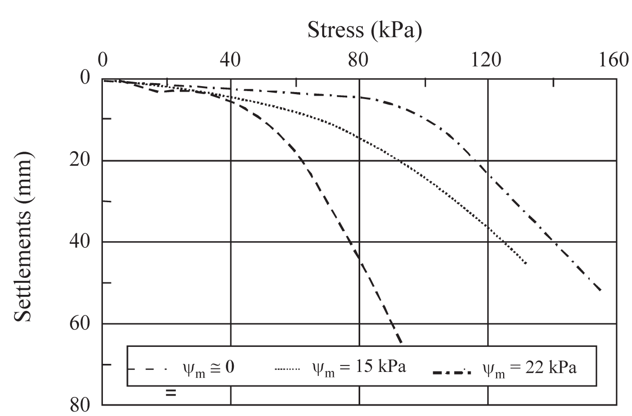

Figure 6 - Stress *vs.* settlement curves of plate load tests on collapsible soil for different levels of matric suction (Costa, 1999).

In order to evaluate the simultaneously influence of the size of the shallow footings, particularly the ones with small sizes, and of the matric suction on the behavior of the shallow foundations in collapsible sandy soil, this work presents a research that was conducted at the Foundations Experimental Site of USP/São Carlos.

Load tests were performed on plates of three different diameters (0.20; 0.40; and 0.80 m) and in footings with 1.50 m diameter, installed in different holes, 1.50 m deep. The tests were conducted under two conditions: a) with no flooding of the area and with the matric suction monitored using tensiometers; b) with the area pre-flooded, in order to represent the diminishing matric suction condition which is inherent to the collapse scenario.

2. Foundations Experimental Site

The representative geotechnical-geologic profile of the Experimental Foundation Site of USP/São Carlos presents a superficial layer, characterized by brown clayey sand, 6 m thick. The action of weathering under weather conditions typical of tropical regions caused the process of laterization. The resulted material is very porous and collapsible. A line of quartz pebbles and limonite separates the superficial layer of the residual soil at a depth of approximately 6 m. The residual soil is constituted by reddish clayey sand, originated from sandstone of the "Bauru Group". The level of the water table varies in between 7 to 10 m deep, depending on the season.

Geotechnical information of this Experimental Site is summarized in Fig. 7. The average value of the standard penetration resistance N_{SPT}, obtained from various campaigns, performed in different times of the year, does not exceed 4 blows/30 cm on the most superficial layer. The void ratio reaches a value close to 1.2 on the surface and tends to decrease with the depth. Regarding the stresses, a practically linear increase is observed in geostatic stress with the depth, due to a small variation of the unit weight. It is also possible to observe that the pre consolidation stress tends to reduce when it goes from non-flooded soil (σ_{po}) to flooded soil condition (σ^*_{po}), which is a common behavior of the collapsible lateritic soils of the Southeast region of Brazil.

3. Tests Performed

Fourteen static plate load tests were performed on rigid metallic circular plates of three different diameters (0.20; 0.40; 0.80 m), and on reinforced concrete footings with circular base with 1.50 m diameter. All elements were installed 1.50 m deep, in different holes with 0.50; 0.60; 0.90 and 1.70 m diameters.

In five tests, the area was pre-flooded for at least 48 h, always maintaining a water layer of at least 50 mm at the bottom of the hole. These tests are represented by codes F-20, F-40, F1-80, F2-80 and F-150, where the letter "F" refers the flooded condition and the numbers refer to the plate or footing diameter, in centimeters.

For the other nine tests performed with no flooding, in different seasons throughout the year, tensiometers were installed at the bottom of the hole in order to monitor the matric suction during the test. Table 1 shows the average matric suction values obtained in the non-flooded tests. The letter "N" refers to the non-flooded condition and the numbers indicate the plate or footing diameter, in centimeters.

The plate load tests were performed according to the NBR-6489 (1984) with the execution methodoly adapted from the quick method of loading (QML) from NBR 12131/91, but with stages that lasted 15 min. The settlement readings were obtained at 0, 1, 2, 3, 6, 9, 12 and 15 min, in each stage, and the unloading was performed in two stages of 15 min. Before unloading the test, there was no maintained load until simultaneous stabilization of load and settlement.

Figs. 8 to 11 show the stress *vs.* settlement curves obtained in all of the plate load tests. The values in brackets correspond to the average matric suction for each test, in kPa.

4. Analyses of the Results

4.1. Bearing capacity

The stress *vs.* settlement curves in Figs. 8 to 11 present the same pattern, characterized by a final stretch that shows an almost linear relationship between settlement and the corresponding applied stress. However, these curves do neither demonstrate a clear rupture nor the evidence a physical rupture. Thus, it is necessary to apply conventional rupture criteria in order to evaluate the bearing capacity of the plate-soil system.

Five criteria were considered as listed bellow:

1. Terzaghi (1943): this criterion states that the bearing capacity of the plate-soil system corresponds to the point from which the stress *vs.* settlement curve starts to show a linear behavior on its final stretch.

Table 1 - Average matric suction in the non-flooded plate load tests.

Plate load tests code	Plate/footing diameter *B* (m)	Matric suction ψ_m (kPa)
N1-20	0.20	15
N2-20	0.20	18
N1-40	0.40	13
N2-40	0.40	12
N1-80	0.80	15
N2-80	0.80	22
N3-80	0.80	33
N1-150	1.50	21
N2-150	1.50	23

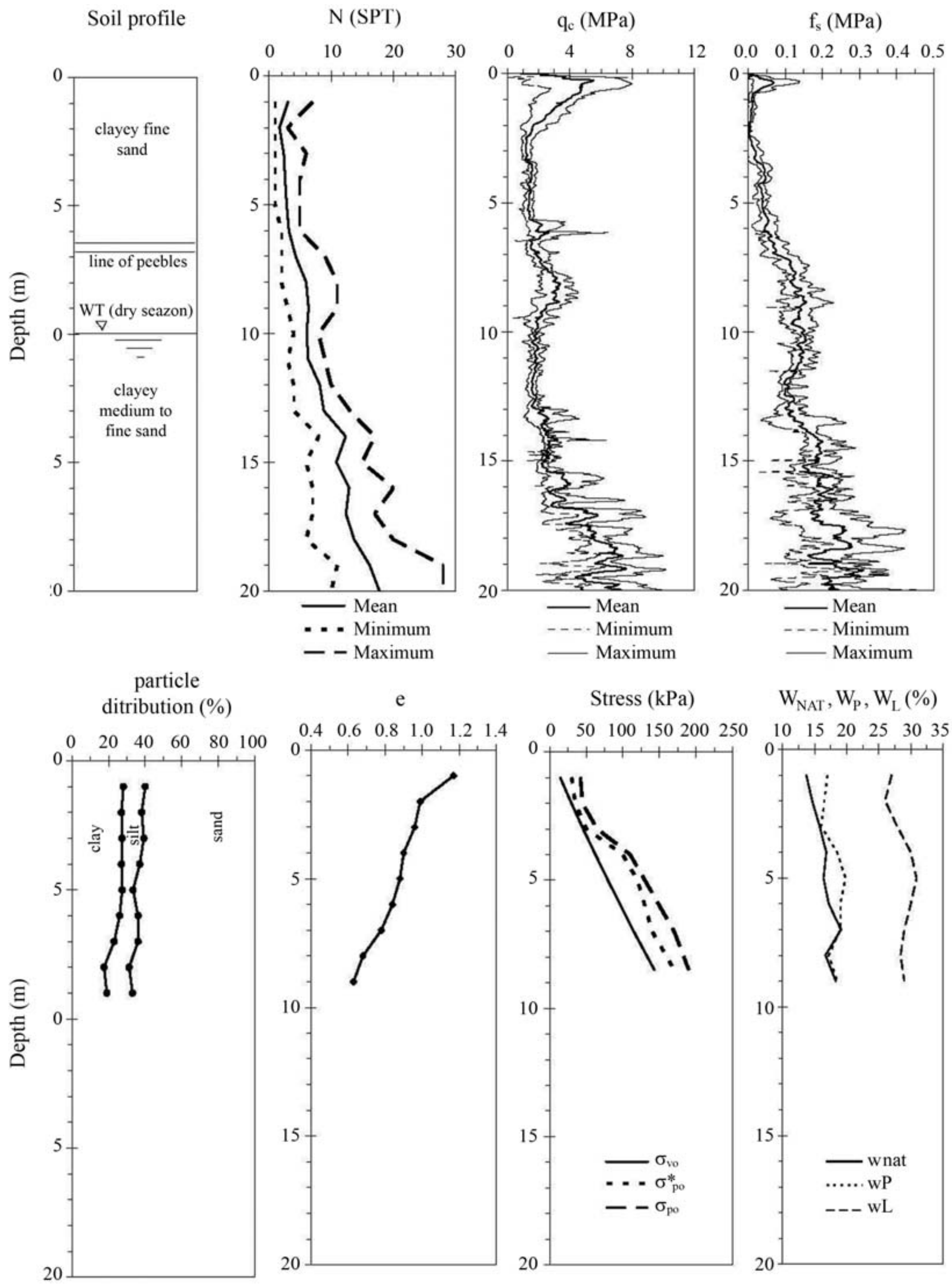

Figure 7 - Geotechnical characteristics of the foundations experimental site of USP/São Carlos (adapted from Menegotto & Vianna, 2000; Giachetti, 2001).

2. Leonards (1962): in this criterion, the bearing capacity is given by the intercepting point of the two tangents, one at the initial portion of the curve and the other at the final portion.

3. "Pre-consolidation" stress: according to the procedure adopted by Macacari (2001), this criterion consists in converting the stress axis to the logarithmic scale and applying the Pacheco Silva method (1970). This is possible due to the similarity of the curves obtained in the plate load tests with the log stress curves *vs.* void ratio of saturated clays consolidation tests.

4. Settlement equal *B*/10 or 10% *B* (Terzaghi, 1942): the bearing capacity corresponds to the stress correspondent to the settlement equal to 10% of the diameter of the plate.

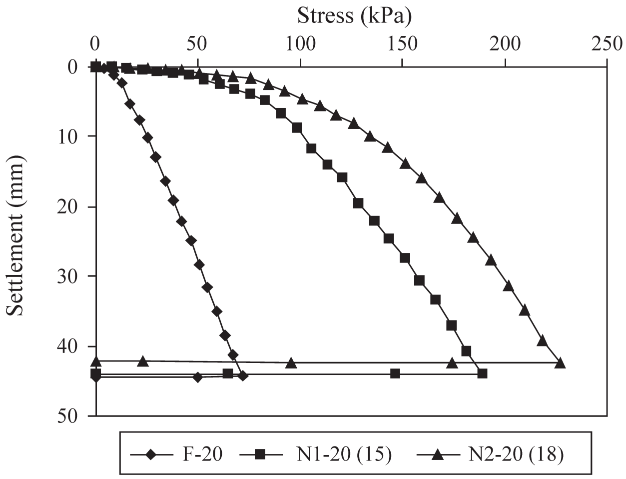

Figure 8 - Stress *vs.* settlement curves of one flooded test and two non-flooded tests (0.20 m diameter plate).

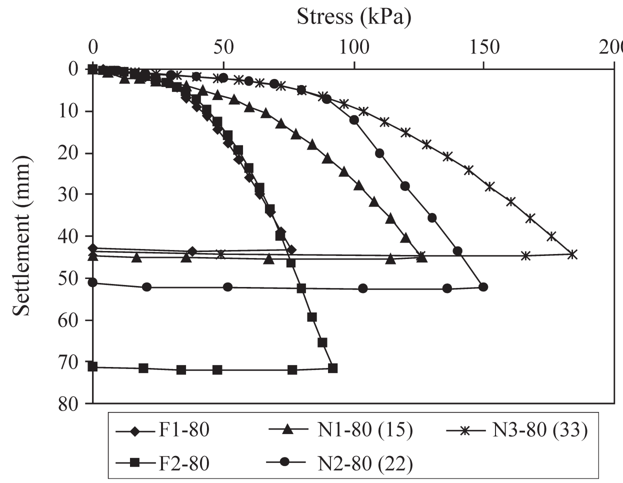

Figure 10 - Stress *vs.* settlement curves of two flooded tests and three non-flooded tests (0.80 m diameter plate).

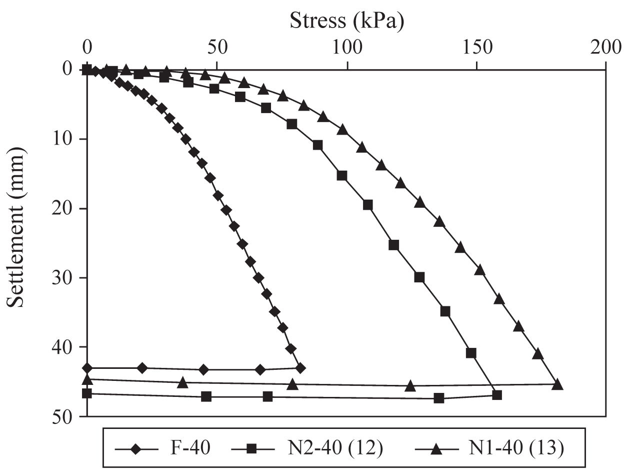

Figure 9 - Stress *vs.* settlement curves of one flooded test and two non-flooded tests (0.40 m diameter plate).

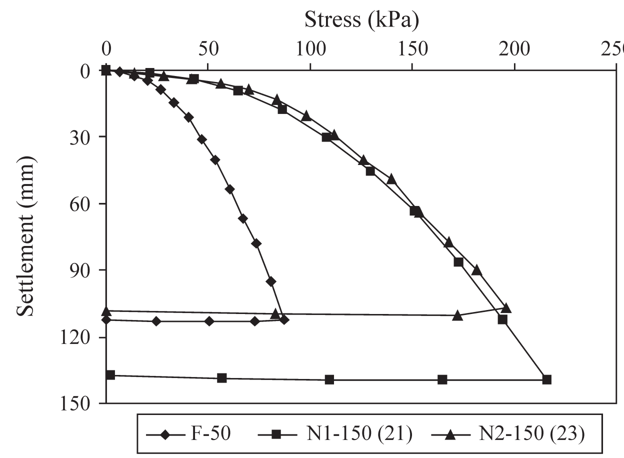

Figure 11 - Stress *vs.* settlement curves of one flooded test and two non-flooded tests (1.50 m diameter footing).

5. Settlement equal *B*/30: the bearing capacity corresponds to the stress correspondent to the settlement equal to 30% of the diameter of the plate (approximately 25 mm, particularly for the plate with diameter *B* = 0.80 m).

Since the application of these different criteria resulted in values reasonably similar, this work presents only the analysis correspondent to the Terzaghi criterion (1943), which is specific to the pattern of curves obtained in this research. The other four analyses may be checked out in Vianna (2005). In particular, the analysis referring the criteria of 10% *B* was published by Vianna *et al.* (2004).

Table 2 shows bearing capacity values (σ_r) obtained in all tests according the conventional rupture criterion by Terzaghi (1943), as well as corresponding values of settlement (ρ_r).

When the bearing capacity values are determined, the values of applied stress may be made dimensionless in the tests dividing the applied stresses by the bearing capacity. The values of settlement may also be normalized dividing them by the plate or footing diameter. Therefore, the stress *vs.* settlement curves are dimensionless for the 14 tests, which are shown in Fig. 12.

It is possible to observe that the dimensionless curves do not show any tendency of converging to a single curve, which implies the existence of the scale effect, in this case.

4.2. The matric suction influence

The behavior of the plate-soil system (or footing-soil) with the variation of the matric suction may be analyzed from the results shown in Figs. 8 to 11.

In terms of deformability, if the curves obtained for plates with the same diameter are compared, it is possible to observe that the settlement for a certain level of stress decreases proportionally with increasing measured matric suction during the plate load tests. It is as if the soil gained an increase of stiffness with the matric suction increase.

As for the resistance of the system, it is possible to observe that the greater the matric suction acting on the soil, the greater the bearing capacity, when tests on plates of the same diameter are compared. Correlating the values of the bearing capacity (σ_r) with the respective values of the matric suction (ψ_m), both values in kPa, it is possible to obtain a reasonably linear variation for each plate diameter as depicted in Fig. 13. The equations resultanting from linear regression analyses are presented in Table 3.

In these four straight-line equations, the angular coefficient varies between 2.3 and 8.6, which is compatible with the calculations by Fredlund & Rahardjo (1993), presented in Fig. 5, where the angular coefficient is 5.

Table 2 - Values of bearing capacity and settlement obtained using Terzaghi criteria (1943).

Test	Bearing capacity σ_r (kPa)	Settlement ρ_r (mm)
F-20	25	10
N1-20	144	25
N2-20	185	24
F-40	54	20
N1-40	144	26
N2-40	109	19
F1-80	56	22
F2-80	68	34
N1-80	102	28
N2-80	100	12
N3-80	144	24
F-150	54	40
N1-150	151	64
N2-150	140	49

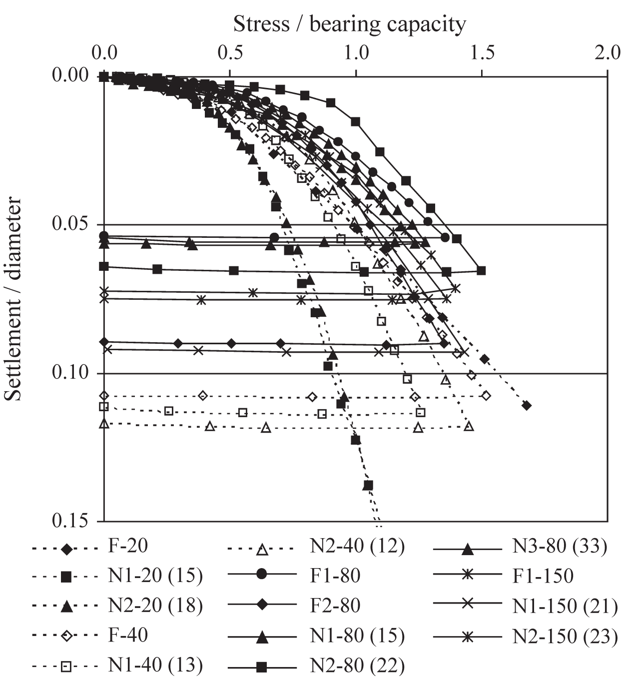

Figure 12 - Dimensionless stress *vs.* settlement for the 14 plate load tests.

4.3. Influence of the plate size on the bearing capacity

Figs. 8 to 11 show that the bearing capacity varies simultaneously with the plate size (or footing size) and with the matric suction. Only for the flooded soil condition, or for suction practically null, it is possible to make a direct analysis of the exclusive influence of the plate or the footing diameter on the bearing capacity. Therefore, considering only the flooded tests, Fig. 14 is obtained, which shows the variation of the bearing capacity with the diameter.

It is possible to observe in Fig. 14 a significant increase of the bearing capacity from a diameter of 0.20 m to 0.40 m. However, the variation of the bearing capacity changes very little between diameters of 0.40 m and 1.50 m.

In order to complement that graph an additional data point could be included corresponding to the diameter of

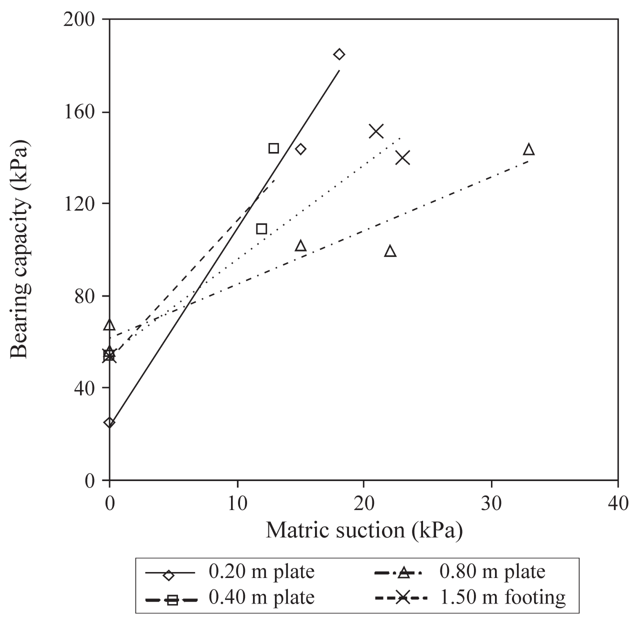

Figure 13 - Variation of the bearing capacity in relation to the matric suction for each plate or footing.

Table 3 - Correlations between bearing capacity σ_r (kPa) and matric suction ψ_m (kPa).

B (m)	$\sigma_r = f(\psi_m)$	R^2
0.20	$\sigma_r = 8.6\ \Psi_m + 24$	0.991
0.40	$\sigma_r = 5.9\ \Psi_m + 53$	0.897
0.80	$\sigma_r = 2.3\ \Psi_m + 61$	0.937
1.50	$\sigma_r = 4.1\ \Psi_m + 55$	0.967

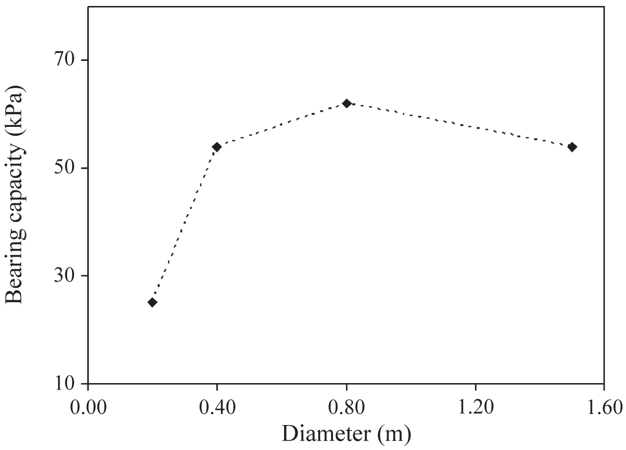

Figure 14 - Bearing capacity *vs.* diameter (flooded tests).

only 28.4 mm. This is the tip diameter of a manual penetrometer utilized by Tshua (2003) and Tsuha *et al.* (2004), for which a resistance of 482 kPa is obtained, in the same place, at the same depth, in the flooded soil condition. Therefore, the bearing capacity obtained with the penetrometer, whose diameter is around 50 times smaller than the tested footing, is approximately nine times greater than that found in the footing load test, with flooded soil. This is coherent with the empiric correlations existing in literature, in which the cone's tip resistance (static penetration test) is always much greater than the bearing capacity of shallow foundations.

For the non-flooded tests it is not possible to make such an analysis directly, because there are no results for different diameters with the same matric suction value.

With the correlations in Table 3 it is possible to calculate the bearing capacity for each plate diameter varying the matric suction values, for example from 0 to 30 kPa in 10 kPa increments. These values calculated for the bearing capacity are presented in Table 4, where the values obtained for the portable penetrometer (B = 28 mm) are included, and for which the following correlations is valid:

$$\sigma_r = 26\,\Psi_m + 482 \tag{4}$$

with R^2 = 0,960 (Tsuha, 2003).

In the same way, Fig. 15 is obtained, which presents the bearing capacity variation with the plate or footing diameter, for each matric suction level (ψ_m).

It is possible to observe in Fig. 15 that, except for the flooded soil case, initially the bearing capacity decreases with the diameter increase, which is consistent with what was demonstrated by De Beer (1965) in Fig. 2. Actually, the corresponding curve to the flooded soil presents a significant similarity with the experimental curve, presented in Fig. 14.

For the 10 kPa curve, the bearing capacity is basically constant up to a diameter of 0.5 m. From this point on, the behaviour is similar to those of the 20 kPa and 30 kPa curves. Only above a diameter of 0.80 m, the bearing capacity may increase with the plate or footing size and this increase is more significant the greater the matric suction is. Coincidently, this is the plate diameter adopted by the Brazilian Standard NBR 6489. This figure proves that this was a correct choice regarding establishing this diameter for plate load tests for foundations design purposes.

In Table 4 it can be noted that the values obtained for the portable penetrometer are the highest ones, since these occur with the results of the cone penetration tests (CPT), as opposed to the shallow foundations bearing capacity values.

4.4. The influence of plate size on the settlements

From the stress *vs.* settlement curves that were obtained in flooded tests, it is possible to obtain the settlement

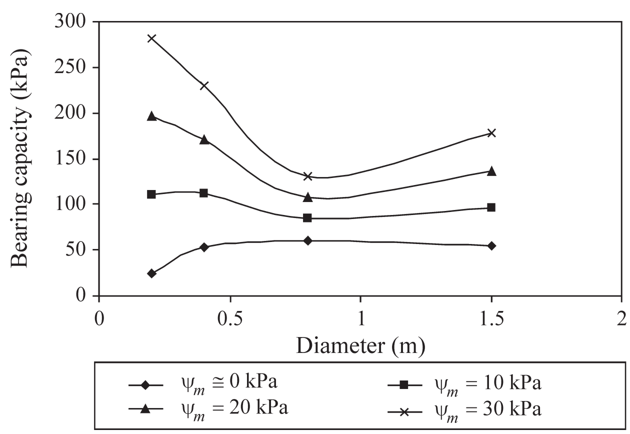

Figure 15 - Variation of the bearing capacity with the diameter, for different matric suction levels.

Table 4 - Calculated values of the bearing capacity for different levels of the matric suction.

Matric suction ψ_m (kPa)	Bearing capacity σ_r (kPa)				
	B = 28 mm	B = 0.20 m	B = 0.40 m	B = 0.80 m	B = 1.50 m
0	482	24	53	61	55
10	742	110	112	84	96
20	1002	196	171	107	137
30	1262	282	230	130	178

values corresponding to several stress levels, for example from 10 to 70 kPa in 10 kPa increments. Therefore, it is possible to establish, for the flooded tests, the influence of the plate diameter on the settlements, for each level of stress, as shown by the curves in Fig. 16.

It is possible to observe that these curves reproduce the pattern shown in Fig. 4, particularly its BF segment. A diameter smaller than 0.20 m, for example 0.10 m, could represent point A of that figure. Therefore, the settlements initially are decreasing as the diameter increases, up to *B* around 0.60 m. From this point on, the settlements begin to increase with the increase of *B* and this growth is more significant as the applied stress increases. This demonstrates the non-linear behaviour of the settlements with the foundation diameter.

For non-flooded tests it is not possible to make a direct analysis of the influence of the plate size on the settlements, because there are no tests with different sizes and the same matric suction. Because of that, a specific procedure was adopted in order to estimate this influence. The values of bearing capacity were calculated for each diameter, utilizing the equations in Table 3 and matric suction values of 10 kPa, 20 kPa and 30 kPa. Afterwards, these points were marked on the graphs of Figs. 8 through 11 and a new curve "parallel" to the existing curves in the graphs was drawn by hand, corresponding to the matric suction adopted values. Then, for each adopted level of matric suction, settlement variation versus plate diameter curves were found for different levels of stress, as shown in Figs. 17 through 19.

Again, it is possible to see the same shape of part of Fig. 4, now using the portion from an intermediate point between *B* and C until F. With other tests, with diameters smaller than 0.20 m, points A and B would probably be defined. In the absence of these points, it is possible to observe on the three figures a certain settlements consistency between diameters 0.20 m and 0.40 m. Between 0.40 m and 0.80 m the settlements increase as *B* increases. For *B* grater then 0.80 m there is a less significant settlement increase for *B* greater than 0.80 m. The curve shape is not affected by the matric suction, but the changes in the settlements will be more pronounced at higher stress levels, as the applied stress increases, for the same matric suction.

5. Allowable Bearing Capacity

Disregarding the tests on smaller plates, it may be considered that the tests on the 0.80 m plate, the Brazilian Standard one, were performed for the purpose of determining the allowable bearing capacity for the 1.50 m footing design.

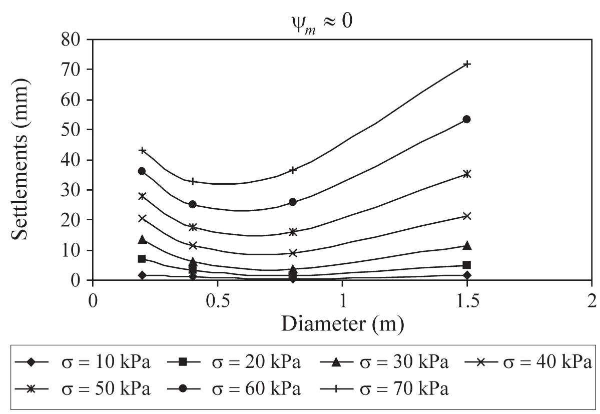

Figure 16 - Variation of the settlement with the plate diameter for different levels of stress (flooded tests).

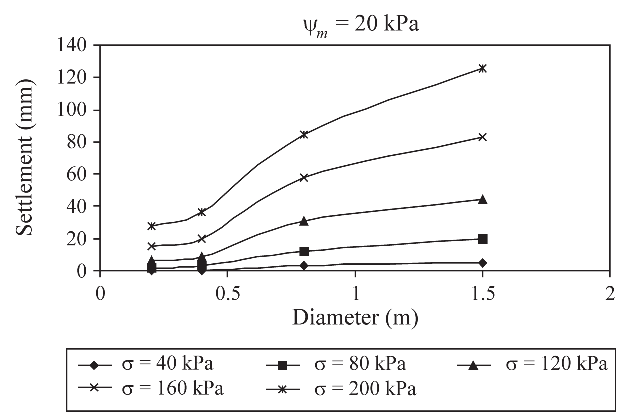

Figure 18 - Variation of the settlement with the diameter for different levels of stress (matric suction of 20 kPa).

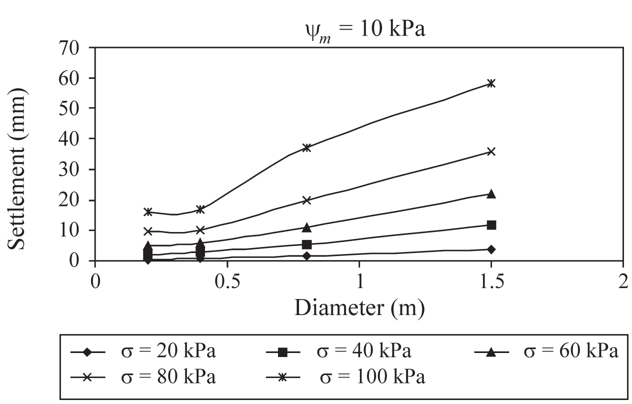

Figure 17 - Variation of the settlement with the diameter for different levels of stress (matric suction of 10 kPa).

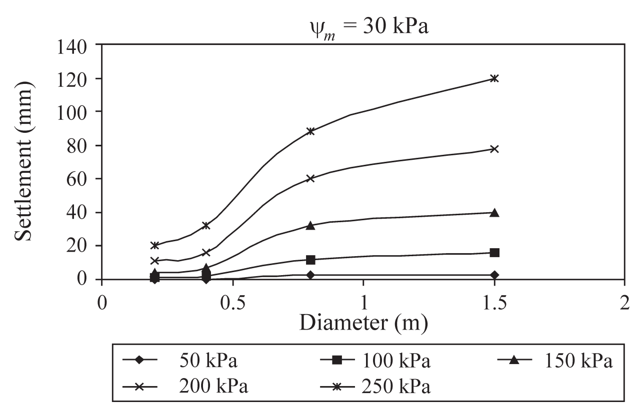

Figure 19 - Variation of settlement with the diameter for different level of stress (matric suction of 30 kPa).

This is a hypothetical case, since the use of shallow foundations on this collapsible soil would demand a soil treatment, through compaction for example (Souza *et al.*, 1995). Nevertheless, this is a very interesting analysis in order to explain the problem of foundation design on collapsible soil. In order to achieve this, two scenarios will be shown, considering or not the soil collapsibility in the design.

5.1. Analyses considering collapsibility

In order to consider the soil collapsibility in the design it is necessary to perform at least one plate load tests with pre-flooding, besides the plate load tests without flooding.

In order to interpret the non-flooded tests stress *vs.* settlement curves, the Boston criterion is used. By this criterion the allowable bearing capacity (σ_a) is given by the smallest of two values: the stress that causes the 10 mm settlement (σ_{10}) and half of the stress corresponding to the 25 mm settlement ($\sigma_{25}/2$). According to Teixeira & Godoy (1996), this criterion stablishes for the plate an admissible settlement of 10 mm and a conventional rupture criterion in which the bearing capacity (σ_r) is associated with the 25 mm settlement. The denominator 2 corresponds to a safety factor.

For the plate load tests performed with soil flooding, the same criterion is used, but the safety factor is 1.5 instead of 2, according to the methodology proposed by Cintra (2004).

Table 5 presents values obtained for the allowable bearing capacity (σ_a), up to the next nearest multiple of 10 in kPa, as well as the corresponding values for settlement (σ_n for non flooded tests; σ_f for flooded tests).

Therefore, even if only one non-flooded test had been performed and only one flooded, the conclusion would still be the same, an allowable bearing capacity of 40 kPa, which is the smallest value found. This allowable bearing capacity of 40 kPa would generate on the plate maximum settlements of 7.3 or 8.8 mm, for the extreme situation of soil flooding.

With this allowable bearing capacity value, the stress *vs.* settlement curves of the plate load tests performed on the footings (N1-150, N2-150 and F-150) shown in Fig. 11, indicate that the footing settlement would be 3.8 mm for the non-flooded tests (matric suctions corresponding to 21 and 23 kPa), but it would increase to 21.0 mm if soil flooding takes place.

5.2. Analyses not considering the collapsibility

Without taking into consideration the soil collapsibility on the footings design, the load tests would not be performed on plates with soil flooding. This would result in higher values of allowable bearing capacity. According to Table 5, in this case one of these three values of allowable bearing capacity would be obtained: 50, 60 or 70 kPa, depending on if the test sample would coincide with N1-80, N2-80 or N3-80, respectively. The corresponding settlement would be totally acceptable (less than 7 mm in any of the tests).

However, if there was a soil flooding, the settlement would increase significantly, which could be quantified with the introduction of those values for allowable bearing capacity on the curves for the flooded tests (F1-80 or F2-80) in Fig. 10. The plates's settlements would be around 14, 24 and 37 mm, respectively, for stresses of 50, 60 and 70 kPa. Therefore, the problem would become even more serious if the allowable bearing capacity is defined based on plate load tests performed in seasons of less humidity (higher matric suction).

This conclusion is confirmed for the footing. When one of these three values for allowable bearing capacity is applied to the stress *vs.* settlement curve of the flooded test (F-150), in Fig. 11, the corresponding settlements of 34, 54 and 70 mm are obtained. Therefore, it is confirmed the seriousness of the problem generated by foundation designs on collapsible soils that do not take in consideration soil collapsibility. Without this consideration, the soil flooding occurrence causes settlements of unacceptable magnitude.

6. Conclusions

Results obtained in 14 plate load tests with metal plates of three different diameters (0.20 m to 0.80 m) and with footings of reinforced concrete of 1.50 m diameter, installed 1.5 m deep, at the Foundations Experimental Site USP/São Carlos were analysed. These results drew important conclusions about the role of the matric suction and about the influence of the diameter on the bearing capacity, as well as on shallow foundations settlements.

Table 5 - Allowable bearing capacity and corresponding settlement.

Test	Matric suction Ψ_m (kPa)	Allowable bearing capacity σ_a (kPa)	Settlement σ_n (mm)	Settlement σ_f (mm)
N1-80	15	50	6.5	–
N2-80	22	60	2.8	–
N3-80	33	70	3.8	–
F1-80	≈ 0	40	–	7.3
F2-80	≈ 0	40	–	8.8

The greater the matric suction acting in the soil, the greater the system's bearing capacity, regardless of the plate or the footing diameter (*B*). For each tested diameter, a linear correlation was established between the matric suction (Ψ_m) and the bearing capacity (σ_r).

The stress *vs.* settlement curves obtained in the plate load tests also show higher values of matric suction result for smaller settlements, regardless of stress level and diameter. On the other hand, decreasing the matric suction to nearly zero induces significant increases in settlements. Therefore, there is no doubt that the matric suction is a factor that cannot be neglected in the bearing capacity analysis and on the settlement of shallow foundations on unsaturated soils.

Using these results it was possible to plot curves in order to define the bearing capacity variation with the diameter. It was found that at lower diameters the bearing capacity decreases as the diameter increases until a minimum bearing capacity value is reached at a diameter of 0.80 m. After this point the bearing capacity increases with increasing plate diameters or footing sizes. This increase is more significant when the matric suction is greater. Therefore, for the research conducted in this type of unsaturated sandy soil, it is unrealistic to consider that the bearing capacity is increasing linearly with the plate or footing diameter, as assumed by the theoretical formulations of shallow foundations bearing capacity.

Curves were also generated for the variation of the settlement with the diameter, for different levels of applied stresses. In the non-flooded tests, a certain consistency of settlements was observed between diameters of 0.20 m and 0.40 m. For *B* between 0.40 m and 0.80 m there is an increase in settlements with an increase in *B*. For *B* greater than 0.80 m there is a less significant increase in the settlements. The curve shape was not affected by the matric suction, but it was much more pronounced with the applied stress increase, for the same matric suction.

For the flooded tests, it was observed that the settlements initially decrease with increasing diameter, up to *B* around 0.60 m. From this point onward, the settlements start to increase with an increase of *B* and this increase is more significant when the applied stress is greater. This work demonstrates that for each level of stress, the settlement variation is very non-linear and always increases with the diameter.

For the hypothesis of the tests on the 0.80 m diameter plate performed for 1.50 m footing design, the conclusion is that performing plate load tests in flooded soil condition is essential in order to determine the allowable bearing capacity.

According to the methodoloty proposed by Cintra (2004), which includes a safety factor of 1.5 for the bearing capacity obtained in the flooded test, the allowable bearing capacity would be 40 kPa. The settlements on footings corresponding to this stress would be 3.8 mm (for an average matric suction of 22 kPa) and they would increase to 21.0 mm in case of soil flooding.

However, if the design was conducted without the soil collapsibility consideration, and therefore without flooded test results, the allowable bearing capacity would vary from 50 to 70 kPa, depending on the season in which the non-flooded test was performed, *i.e.*, depending on the matric suction acting on the soil on the test day. For these values of allowable bearing capacity, the settlements on footings would increase to 34 to 70 mm if soil flooding occurs.

References

ABNT (1984) Bearing Capacity Tests on Foundation Ground. Brazilian Standard NBR 6489, Rio de Janeiro, 2 pp. (in Portuguese).

ABNT (1991) Piles - Static Load Tests. Brazilian Standard NBR 12131, Rio de Janeiro, 4 pp. (in Portuguese).

Cintra, J.C. (1998) Foundations on Colapsible Soils. Rima Editora, São Carlos, 106 pp. (in Portuguese).

Costa, Y.D. (1999) A Study on the Behaviou of an Unsaturated Soil in Plate Load Tests. MSc. Thesis, Escola de Engenharia de São Carlos, Universidade de São Paulo, São Carlos, 131 pp. (in Portuguese).

Costa, Y.D.; Cintra, J.C. & Zornberg, J.G. (2003) Influence of matric suction on plate load test result performed on lateritic soils. Geotechnical Testing Journal, v. 26:2, p. 219-227.

Cintra, J.C.A. (2004) Soil mechanics applications - Foundations on colapsible soils. V Brazilian Symposium on Unsaturated Soils, São Carlos, v. 2, p. 575-593 (in Portuguese).

Cintra, J.C.A.; Macacari, M.F.; Aoki, N. & Vilar, O.M. (2005) Variations of bearing capacity with matric suction and depth in plate load tests on colapsible soil. Soils and Rocks, v. 28:1, p. 21-29 (in Portuguese).

De Beer, E.E. (1965a) Bearing capacity and settlement of foundations. Symposium on Bearing Capacity and Settlement of Foundations. Heald at Duke University, Durham, p. 15-34.

Fredlund, D.G. & Rahardjo, H. (1993) Soil Mechanics for Unsaturated Soils. John Wiley & Sons, New York, 517 pp.

Gorbunov-Possadov, M.I. & Davidov, S.S. (1973) Interaction of soil bases and structures (Prediction of settlement, design of massive foundations based on the limiting state, design of flexible foundation beams and slabs). VIII International Conference on Soil Mechanics and Foundation Engineering, Moscow, v. 3, p. 46-92.

Giacheti, H.L. (2001) *In Situ* Tests and Their Applications to Tropical Soils. Thesis, Universidade Estadual Paulista, Bauru, 299 pp. (in Portuguese).

Leonards, G.A. (1962) Foundation Engineering. McGraw-Hill, New York, 1136 pp.

Macacari, M. (2001) Variations of Bearing Capacity with Suction and Depth in Plate Load Tests on Tropical Soil. MSc. Thesis, Escola de Engenharia de São Carlos, Universidade de São Paulo, São Carlos, 96 pp.

Menegotto, M.L. & Vianna, A.P.F. (2000) *In situ* tests in the experimental foundation site of EESC-USP. Internal Report, Escola de Engenharia de São Carlos, Universidade de São Paulo, São Carlos, 30 pp. (in Portuguese).

Pacheco Silva, F. (1970) A new graphic construction method for the determination of the overconsolidation pressure of a soil sample. IV Brazilian Conference on Soil Mechanics and Foundation Engineering, Rio de Janeiro, v. 2, p. 219-224. (in Portuguese).

Souza, A.; Cintra, J.C.A. & Vilar, O.M. (1995) Shallow foundations on collapsible soil improved by compaction. 1st International Conference on Unsaturated Soils, Paris, v. 2, pp. 1017-1021.

Teixeira, A.H. & Godoy, N.S. (1996) Analysis, design and construction of shallow foundations. Foundations: Theory and Practice, Hachich *et al.* (editors), Pini Publishers, São Paulo, chapter 7, pp. 227-264. (in Portuguese).

Terzaghi, K. (1942) Discussion on pile driving formulas. Proc. ASCE, 68:2, p. 311-323.

Terzaghi, K. (1943) Theoretical Soil Mechanics. John Willey & Sons, New York, 510 pp.

Tsuha, C.H.C.; Cintra, J.C.A. & Aoki, N. (2004) The use of a manual penetrometer in a colapsible soil with suction monitoring. 5° Brazilian Symposium on Unsaturated Soils, São Carlos, v. 1, p. 395-401 (in Portuguese).

Tsuha, C.H.C. (2003) Utilization of a Manual Penetrometer in a Colapsible Soil and Comparisons with Results from Plate and Footing Load Tests. MSc. Thesis, Escola de Engenharia de São Carlos, Universidade de São Paulo, São Carlos, 53 pp. (in Portuguese).

Van Der Veen, C. (1953) The bearing capacity of a pile. III International Conference on Soil Mechanics and Foundation Engineering, Zurich, v. 2, p. 125-151.

Vianna, A.P.F.; Cintra, J.C.A. & Aoki, N. (2004) Influence of size and suction on the bearing capacity of shallow foundation in non-saturated sandy soil. 5th Symposium of Special Foundation and Geotechnique, SEFE V, São Paulo, v. 2, p. 48-56.

Vianna, A.P.F. (2005) Influence of Size and Matric Suction on the Behaviour of Shallow Foundations on Unsaturated Sandy Doil. PhD. Thesis, Escola de Engenharia de São Carlos, Universidade de São Paulo, São Carlos, 170 pp. (in Portuguese).

Algorithm Development for Incorporating Soil Physical Properties of each Different Soil Class in a Landslide Prediction Model (SHALSTAB)

Verônica Moreira Ramos, Renato Fontes Guimarães, Osmar Abílio de Carvalho Junior, André Luciancencov Redivo, Roberto Arnaldo Trancoso Gomes, Fabrício Bueno da Fonseca Cardoso, Nelson Ferreira Fernandes

Abstract. The Shallow Stability Model (SHALSTAB) identifies shallow landslide susceptible areas, combining a steady state runoff model that estimates the topographically induced spatial variation in pore pressures with an infinite slope model for shallow landslides. Although the landslides present a strong topographic control, the variability of the soil properties significantly modifies the model results. Thus, the aim of this study was to develop an algorithm for incorporating soil physical properties for each different soil class in the SHALSTAB model, in order to analyze the influence of these parameters in landslides triggering. This approach allowed the model to have a better performance when compared with SHALSTAB results with constant values of soil properties (simple method). It contributed to a more effective prediction in shallow landslide susceptible areas.
Key words: mathematical modeling, landslides, digital elevation model, SHALSTAB model.

1. Introduction

Landslides are common processes along the mountainous landscape of the Brazilian coast, especially during intense summer rainfalls (Ploey & Cruz, 1979; Fernandes *et al.*, 1994; Lacerda, 1997; Smyth & Royle 2000). These catastrophic phenomena are reported almost every year for causing loss of lives and serious damage to roads, bridges, and properties. This is especially true in major cities such as Rio de Janeiro, Santos, Petrópolis and Salvador. Unregulated peri-urban land development has given rise to complex urban structures, which predominantly spread towards the steep hillslopes inside and around the city. This urbanization, especially the slums, includes lack of basic infrastructure services and a rapid densification of informal settlements. The spatial segregation in the cities is characterized by the convergence of numerous intervening social, economic, cultural and environmental variables aggravated by the lack of appropriate public policies and the stigmatization of social minority groups in the urban space (Wacquant & Wilson, 1989; Paim *et al.*, 1999; Santos *et al.*, 2006).

The structure and dynamics of informal urban growth and land use change natural conditions and slope stability by the extensive use of cuts, deforestation, changes in drainage conditions, accumulation of garbage in deposits, among others (Dietrich *et al.*, 1993; Moeyersons, 2003). Many studies have shown that, in this region, topography plays an important role in controlling the location of landslide scars (Barata, 1969). Thus, it is necessary to establish tools for regulating and directing the development of urban land use in order to minimize an imminent urban crisis caused by landslides. Much of disaster policy still emphasizes the impact of nature, and this has led to the dominance of technical intervention focused on predicting the hazard or modifying its impact.

Process-based models are increasing the focus on erosion and landslide studies and hazard assessments because they allow for spatially explicit examination of the potential effects of changes in the governing hydrological and geomorphologic processes. For this reason, a variety of models have been developed and applied in studies of erosive processes (*e.g.*, Moore *et al.*, 1988) to locate saturation zones (*e.g.*, Beven & Kirkby, 1979; O'Loughlin, 1986, Dietrich *et al.*, 1992; Terlien, 1997) and evaluate areas of a landscape shaped by different geomorphologic processes (*e.g.*, Dietrich *et al.*, 1993). These models have been more and more used in environmental studies, since, besides making an understanding of the environmental changes deriving from inappropriate soil management possible, they can also be used to predict future landscape alterations.

Verônica Moreira Ramos, Lecturer, Departamento de Geografia, Universidade de Brasília, 70910-900 Brasília, DF, Brazil. e-mail: vmramos@unb.br.
Renato Fontes Guimarães, Associate Professor, Departamento de Geografia, Universidade de Brasília, 70910-900 Brasília, DF, Brazil. e-mail: renatofg@unb.br.
Osmar Abílio de Carvalho Junior, Associate Professor, Departamento de Geografia, Universidade de Brasília, 70910-900 Brasília, DF, Brazil. e-mail: osmarjr@unb.br.
André Luciancencov Redivo, MSc. Student, Programa de Pós-Graduação em Geografia, Departamento de Geografia, Universidade de Brasília, 70910-900 Brasília, DF, Brazil. e-mail: andrelredivo@unb.br.
Roberto Arnaldo Trancoso Gomes, Lecturer, Departamento de Geografia, Universidade de Brasília, 70910-900 Brasília, DF, Brazil. e-mail: robertogomes@unb.br.
Fabrício Bueno da Fonseca Cardoso, Secretaria de Recursos Hídricos, Ministério do Meio Ambiente, 70830-901 Brasília, DF, Brazil. e-mail: fabrício.cardoso@mma.gov.br.
Nelson Ferreira Fernandes, Associate Professor, Departamento de Geografia, Instituto de Geociências, Universidade Federal do Rio de Janeiro, Ilha do Fundão, 21945-970 Rio de Janeiro, RJ, Brazil. e-mail: nelsonff@acd.ufrj.br.

Several different methods and techniques for landslide susceptible mapping have been proposed or tested to identify potentially unstable slopes such as: (a) use of a critical slope angle to designate areas of high hazard (Cruz, 1974; Gao, 1993; Zhou *et al.*, 2002), (b) analyses that combine morphological aspects, vegetation, land use, lithology and geotechnical information (Montgomery *et al.*, 1991, Carrara, 1983; Carrara *et al.*, 1991; Gao, 1993; Larsen & Torres-Sanchez, 1998); and (c) an approach which combines a topographically-driven hydrological model with slope stability models to predict areas of high hazard (*e.g.*, Okimura & Ichikawa, 1985; Dietrich *et al.*, 1992; van Asch *et al.*, 1993; Wu & Sidle, 1995; Pack *et al.*, 1998; Iverson, 2000).

The Shalstab (Shallow Stability) model has been used to predict areas subject to shallow landsliding in both urban and rural settings in temperate regions of the western United States (Dietrich *et al.*, 1993, 1995, 2001; Montgomery & Dietrich, 1994; Montgomery *et al.*, 1998) and in tropical Brazil (Guimarães *et al.*, 2003a; Fernandes *et al.*, 2004; Gomes *et al.*, 2005). This approach is based on coupling a hydrological model and slope stability models (Montgomery & Dietrich, 1994; Dietrich & Montgomery, 1998).

The scope of this paper is to identify the landslide susceptible areas of the city of Salvador using the SHALSTAB model, and additionally, to examine the geotechnical properties for different soil classes in the model because, usually, SHALSTAB works with a unique set of soil property over the entire basin. The primary goal is to study spatial geotechnical factors for soil classes that conjointly influence the landslides occurrence. The second goal is to create an algorithm to incorporate spatial distribution of soil properties in the SHALSTAB model. The third goal is to compare these SHALSTAB results with results assuming constant values for the soil properties (simple method).

2. Study Area

The municipality of Salvador is located between the coordinates 12°47' and 13°30' south latitude and 38°18' and 39°30' west longitude in an area of 316 km^2. The study area is located in the northeastern portion of the municipality in a surface of about 9 km^2 that includes most of the district named *Subúrbio Ferroviário de Salvador* (Fig. 1).

The climate in the study area is mostly conditioned by the action of Tropical Unstable Lines (TUL), with the predominance of east winds that reach the coast of Bahia and cause rain, mainly in the summer. The climate of the area is classified as Tropical Humid (TU), with average annual temperature around 24° Celsius and annual precipitation index varying from 1200 to 2000 mm (Magalhães, 1993).

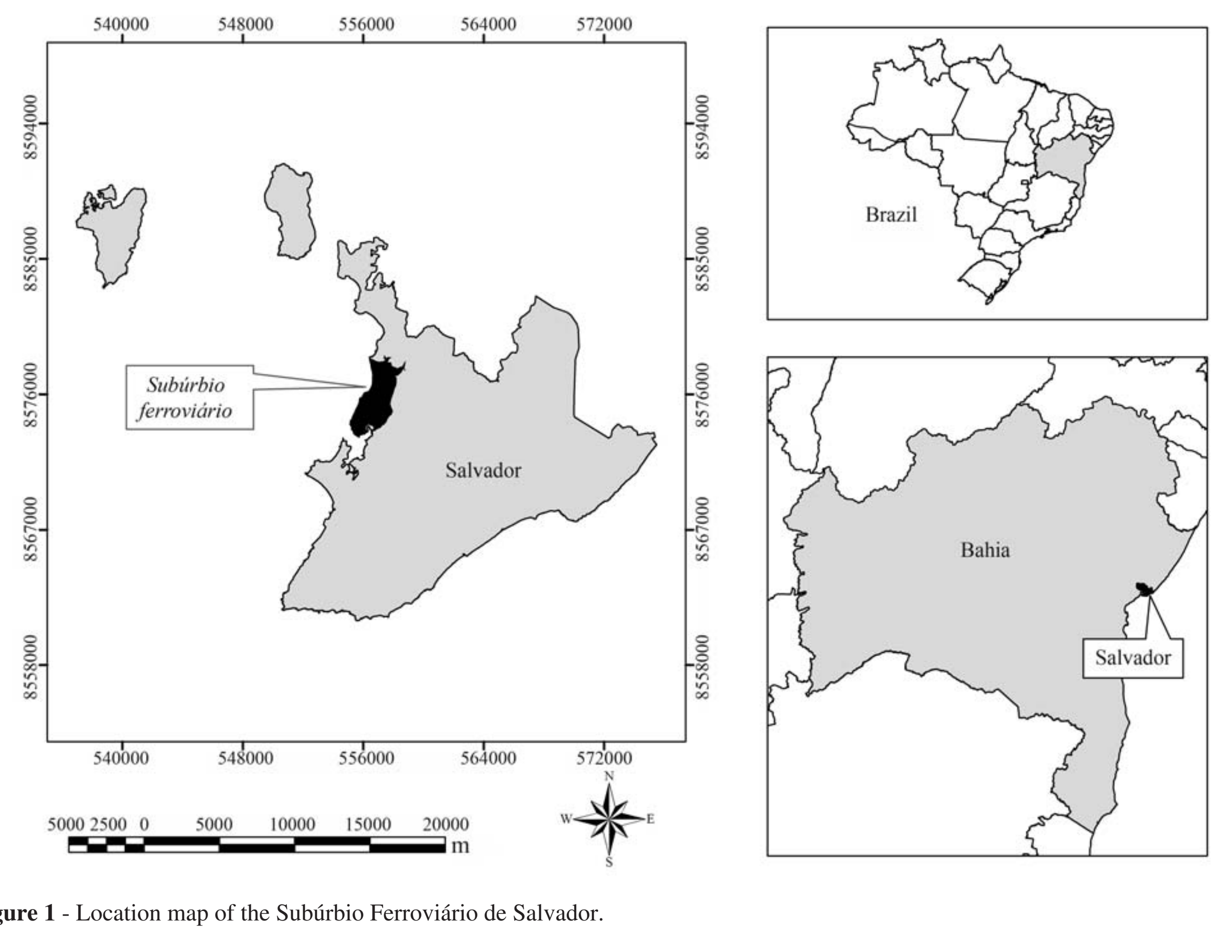

Figure 1 - Location map of the Subúrbio Ferroviário de Salvador.

Geologically, the city of Salvador is mainly represented by: (a) Crystalline Embasement formed by high degree, highly fractured metamorphic rocks (Tricart & Silva, 1968); (b) Recôncavo sedimentary basin terrains, which are abandoned rifts resulting from South Atlantic opening evolution, continental separation between the African and South American (Macdonald *et al.*, 2003), formed predominantly by siltites, shales and sandstones of the Marfim and Pojuca Group in the study area (Geohidro, 1993); and (c) Barreiras Group derived from Tertiary sediments composed of sandstones and conglomerate deposits (Viana *et al.*, 1971; Rossetti & Góes, 2001).

The low strength of the sandy layers of the Barreiras Group sediments results in soil erosion (Viana *et al.*, 1971; Geohidro, 1993). The natural geodynamics presents high susceptibility to landslides due to the pedologic characteristics (intense weathering and vertical variation of the soil profile texture) and extreme climatic events with concentrated rainfall (Peixoto, 1968; Magalhães, 1993). One can observe some spatial erosion patterns in morphology as: (a) the relief has convex hills with high desiccation, occasionally tabular rate; (b) interfluves are generally convex and the fluvial incision gives the concave features; (c) concave shaped slopes are the preferable zones for convergent flux, and they are more susceptible to landslides (Peixoto, 1968). The landslides and gully erosion are commonly triggered or accelerated by human occupation.

The soil occupation in *Subúrbio Ferroviário* occurred in 1875 and is one of the oldest in Salvador (Serpa & Garcia, 1999). However, only from 1950 to 1970 did a large population growth occur, through invasion, with the development of a complex urban structure with predominantly informal urban growth (Brito, 1997). In 1968 the first transference of poor population occurred, due to a governmental policy to withdraw slums from the richer areas of the city. As a result, the *Subúrbio Ferroviário* suffered a dense occupation by popular houses without any planning or environmental adjustment.

Despite Salvador's modernization, concerning urban investments in infrastructure, the city still grows without appropriate planning, mainly in the suburbs. In the *Subúrbio Ferroviário de Salvador*, the slope destabilization caused by deforestation and concentration of informal settlements intensified several environmental and social problems. This is one of the areas in the municipality of Salvador with the highest proportion of landslide victims. As the population increases, the number of houses multiplies and the slums expand intensively on the slopes disregarding its risk factors. The lack of state investments in infrastructure such as waste disposal systems, drainage systems, among others, is clear. Table 1 shows the occurrence and the increment of accidents caused by landslides in Salvador from 1971 to 1999, as well as a considerable social-economic loss.

Table 1 - Mass movement consequences in Salvador between 1971 and 1999 (Source: Augusto Filho & Wole, 1996; Codesal, 2002).

Year	Consequences
1971	104 deaths approximately and thousands of injuries and homeless
1989	109 deaths approximately and many properties damaged
1992	11 deaths approximately, many injuries and properties damaged
1993	5 deaths and many properties damaged
1994	4 deaths, many injuries and more than 150 properties damaged
1995	59 deaths approximately, 48 injuries and more than 500 homeless
1996	29 deaths approximately, many injuries and homeless
1997	10 deaths, approximately 150 homeless and many injuries
1998	3 deaths, many homeless and properties damaged
1999	3 deaths, 50 homeless and many properties damaged

3. SHALSTAB Model

The soil thickness reflects a direct relation between local pedogenesis and erosion (transport) or sedimentation (deposition) and also has a strong interrelation with slope. The relief concave portions (hollows), besides constituting places of high water table, since they represent convergent sites, are also places where the transport material causes sediment accumulation, and consequently, the increase in soil thickness, especially when on unchanneled valleys (Dietrich & Montgomery, 1998).

Dietrich & Montgomery (1998) developed a process-based mathematical model (SHALSTAB model) for the topographic control of shallow landslides. This model results from the combination of a slope stability model with a hydrological model and determines the shallow landslide susceptible areas for each cell (pixel) of the grid (region of interest). Its performance depends basically on both the DEM resolution and the soil physical parameters data.

The slope stability model is based on the concept of an infinite constant slope with constant soil thickness that defines the shear stress on the shear plane (Carson & Kirkby, 1972). The total shear strength at failure is given by Eq. (1):

$$\tau = C' + (\sigma - u)\tan\phi' \tag{1}$$

where τ is the shear strength (kN/m^2), σ is the normal stress (kN/m^2), u is the pore pressure (kN/m^2), C' is the net apparent cohesion attributable to soil cohesion and root reinforcement (kN/m^2) and ϕ' is the effective internal friction angle (degrees).

Figure 2 shows the soil block within the regolith so the value of weight (P) has to be determined indirectly. An approach is to work with the equivalent rectangle ABDF instead of parallelogram ACEF.

Thus, the soil thickness is expressed by Eq. (2):

$$e = z\cos\theta \qquad (2)$$

P can be expressed by Eq. (3):

$$P = L\,\rho_s\, g\, z\cos\theta \qquad (3)$$

where ρ_s corresponds to bulk density of the soil (kg/m^3), L is the block length (m) and g is the gravitational acceleration (m/s^2).

The lateral root strength model shows that greater root strength is more required for the lateral than the infinite-slope model that provides an only one-dimensional model.

Substituting P (Eq. 3) and dropping L, because it is not relevant in an infinite slope analysis, the shear stress (τ) and normal stress (σ) can be expressed by:

$$\tau = \rho_s\, g\, z\cos\theta\sin\theta \qquad (4)$$

$$\sigma = \rho_s\, g\, z\cos^2\theta \qquad (5)$$

Pore-water pressure (u) on the slide plane (Fig. 2), where ρ_w is the bulk density of water (kg/m^3) and h is the thickness of the saturated soil above the impermeable layer (m) is given by:

$$u = \rho_w\, g\, h\, z\cos^2\theta \qquad (6)$$

Under this assumption, Eq. (1) can be expressed by:

$$\rho_s = gz\cos\theta\sin\theta = C' + (\rho_s gz\cos^2\theta - \rho_w gz\cos^2\theta)\tan\phi \qquad (7)$$

According to Montgomery & Dietrich (1994), by solving Eq. (7) considering the ratio h/z, the slope stability model can be represented by Eq. (8):

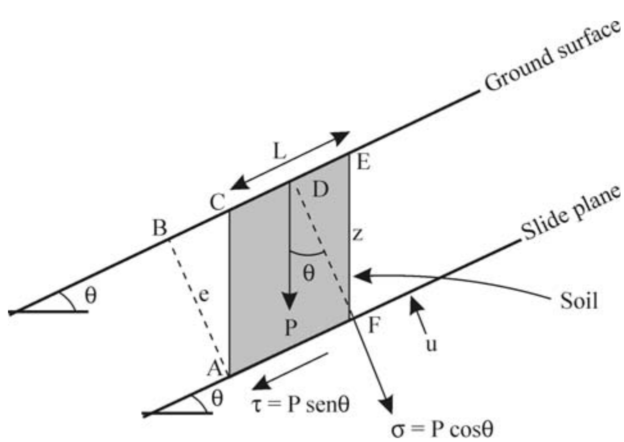

Figure 2 - Stresses acting on a slope of a translational landslide (Adapted from Guimarães *et al.*, 2003b).

$$\frac{h}{z} = \frac{C'}{\rho_w gz\cos^2\theta\tan\phi} + \frac{\rho_s}{\rho_w}\left(1 - \frac{\tan\theta}{\tan\phi}\right) \qquad (8)$$

The hydrological model used by SHALSTAB is based on the methodology developed by O'Loughlin (1986), which maps the spatial saturation pattern from the analysis of the upward contribution area, soil transmissivity and local slope, considering that the subsurface flow is parallel to hillslope. Thus, soil saturation condition in equilibrium can be represented as a function of a local wetness (W), as showed in Eq. (9).

$$W = \frac{Q}{T}\frac{a}{b\sin\theta} \qquad (9)$$

where a is the upwards contribution area (m^2), b is the length across which flow is accounted for (m), T is the soil transmissivity (m^2/day), Q is the rainfall intensity (mm) and θ is the local slope (degrees).

Montgomery & Dietrich (1994) adopted a simplifying assumption that the saturated conductivity of the soil is constant along the soil profile. Thus, local wetness can be expressed by the ratio h/z when $W < 1$, so:

$$\frac{h}{z} = \frac{Q}{T}\frac{a}{b\sin\theta} \qquad (10)$$

This way, combining the infinite stability slope model with the hydrological model, which corresponds respectively to Eqs. (8) and (10), one can predict the critical ratio of the steady-state rainfall to the transmissivity necessary to trigger landslide (Q/T) (Eq. 11):

$$\frac{Q}{T} = \frac{\sin\theta}{(a/b)}\left(\left(\frac{C'}{\rho_w gz\cos^2\theta\tan\phi}\right) + \left(\frac{\rho_s}{\rho_w}\right)\left(1 - \frac{\tan\theta}{\tan\phi}\right)\right) \qquad (11)$$

4. Methodology

The input data for the shallow landslide susceptible areas prediction model (SHALSTAB) are: slope and contribution area obtained for the study area from the resulting Digital Elevation Model (DEM) and the soil parameters.

4.1. Terrain attribute data

A 1-m grid DEM was built from digital contour coverage from a 1:5,000 scale topographic map (Fig. 3) and interpolated using the Topogrid module of ARC/INFO. This procedure employs an algorithm developed by Hutchinson (1989) to create hydrologically sound DEM. The algorithm was designed to produce accurate DEM's with reasonable drainage properties from comparatively low-detail and low-accuracy elevation and streamline data sets. The procedure couples a drainage enforcement algorithm that removes spurious sinks and pits, with a finite difference interpolation technique based on the minimization of a terrain specific, rotation invariant roughness penalty (Hutchinson, 1989). The interpolation algorithm was designed to

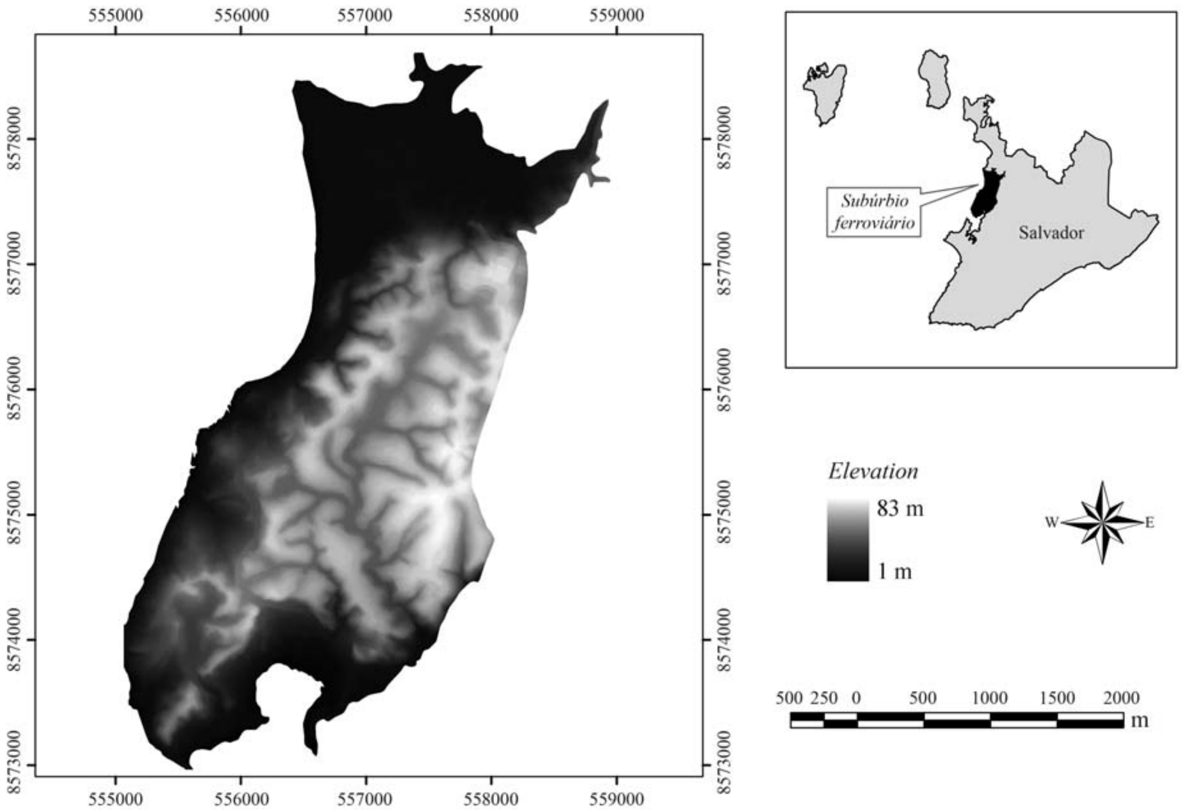

Figure 3 - 1-m grid Digital Elevation Model built from digital contour coverage from a 1:5,000 scale topographic map.

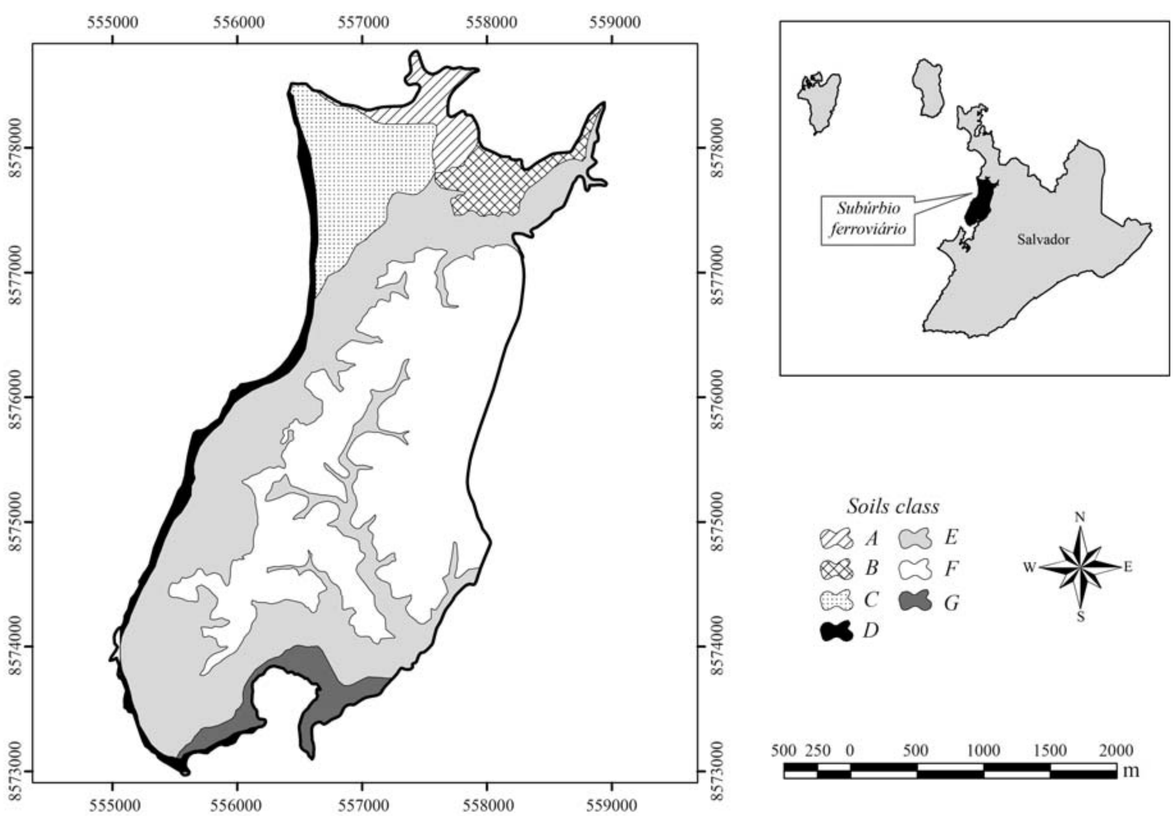

Figure 4 - Soil classes defined for the *Subúrbio Ferroviário de Salvador* (Source: Geohidro, 1993).

have the computation efficiency of local methods (*e.g.* Inverse Distance Weighted) and the continuity in the interpolated surface generated by global methods (*e.g.* Kriging interpolator). In addition, the location and flow direction of the major stream in the valley were digitized and used as extra input for the interpolation procedure.

4.2. Geotechnical properties data

The *Subúrbio Ferroviário* soil map presents seven classes (Geohidro, 1993) (Table 2 and Fig. 4). Classes A, B, C, D and G were grouped as only one class due to the fact that they are located in a gentle relief and, therefore, have the same potential to landslide (Table 3 and Fig. 5).

The geotechnical properties estimate for soil classes (friction angle, cohesion and bulk density) was based on the geotechnical essays developed by Menezes (1987) for three kinds of soils in the Recife urban area with the same characteristics of *Subúrbio Ferroviário de Salvador*.

Table 3 shows the correspondence between the three kinds of slope soils of the Recife urban area with the three kinds defined for *Subúrbio Ferroviário de Salvador* and their respective values of friction angle, cohesion and bulk density.

4.3. Algorithm approach

An algorithm in ARC/INFO Macro Language (AML) was implemented in the SHALSTAB model in order to input cohesion, friction angle and soil density values.

For comparison purposes the SHALSTAB model was also applied disregarding the soil cohesion (simple method) and considering constant values for the friction angle (45°) and soil density (1.700 kg/m^3) (Dietrich & Montgomery, 1998). The b value, which is the cell size (pixel), is also constant for the whole area and equal to 1 m.

Table 3 - Soil parameters (Menezes, 1987).

Soil types	ϕ (degrees)	C (kN/m^2)	ρ (kg/m^3)
A	25	1	1500
B	28	10	1500
C	31	7	1500

Notes: ϕ = Friction angle, C' = Cohesion and ρ = Bulk density.

5. Results

The shallow landslide susceptible area, expressed by the ratio *Q/T*, is demonstrated in Figs. 6 and 7. The bedrocks outcrops are located in the class named unconditionally unstable, as well as the areas where the most abrupt interfluves are found. They are characterized, thus, as landslide susceptible areas, even not being completely saturated. The class named unconditionally stable refers to the areas with low slopes.

The frequency distribution of the shallow landslide susceptibility was observed, both from the algorithm developed and from the simple method, in order to evaluate the spatial variation of the soil physical properties. By analyzing Table 4, one can notice that, for the two simulations carried out, the class considered unconditionally unstable is rather superior than the unconditionally stable one. It reached 92,49% in the simulation by the simple method and 97% in the simulation by the algorithm.

Regarding the other susceptibility classes, the comparison between the two simulations has shown that the al-

Table 2 - Degree of landslide potential obtained after crossing soil classes and local slope.

Soil class	Characteristics	Slope classes (%)					
		0 to 5	5 to 15	15 to 25	25 to 35	35 to 45	45 to 50
A	Composed of fine sand, silt, clay and organic matter. Come up on flood surface	B	M	A			
B	Alluvial deposit composed of fine sand, silty and clayey, low support capacity	B	M	A			
C	Expansive clay, from the alteration of shale, sensitive to humidity variation	B	M	M/A	A		
D	Beach deposit, composed of fine to medium-sized, light gray sand, occurs on the coast	B	M	A			
E	Sandy-silty-clayey, clayey layers, presents good cohesion.	B	B	M	M/A	A	
F	Originates from the Barreiras group. Composed of thick sand and red-gray clay	B	B	B	M	M/A	A
G	Composed of fine to middle-sized sand and organic matter	B	M	A			

Notes: B represents a low degree of landslide potential, M represents a median degree of landslide potential, M/A a median to high level of landslide potential and A represents a high degree of landslide potential (Source: Geohidro, 1993).

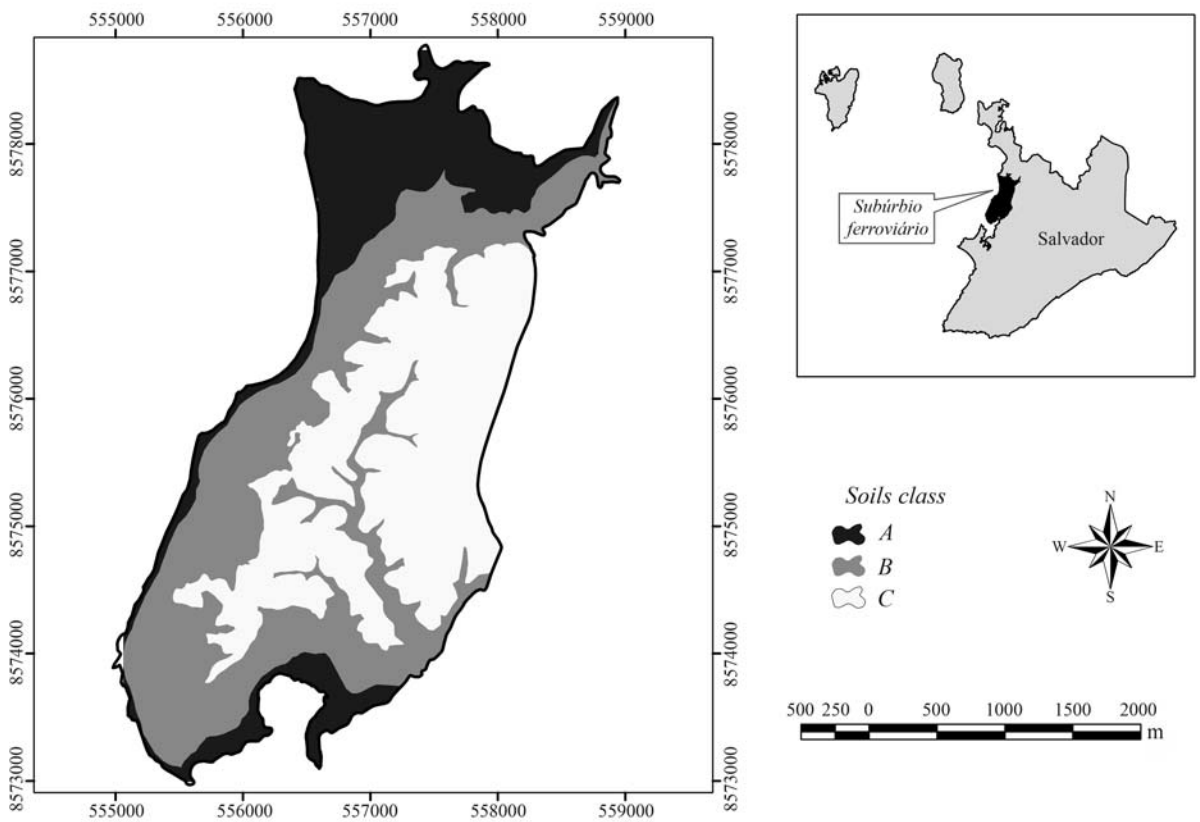

Figure 5 - Soils Map considering the three classes.

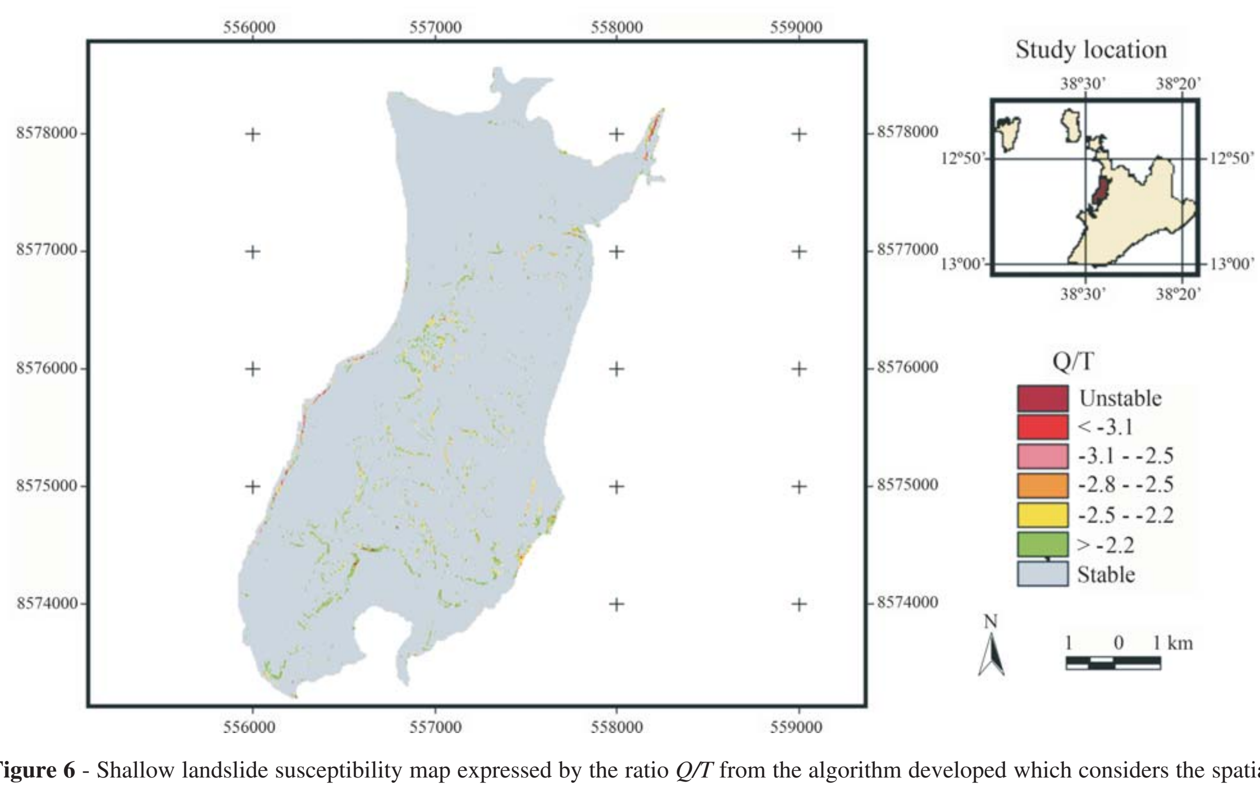

Figure 6 - Shallow landslide susceptibility map expressed by the ratio *Q/T* from the algorithm developed which considers the spatial variation of the soil properties.

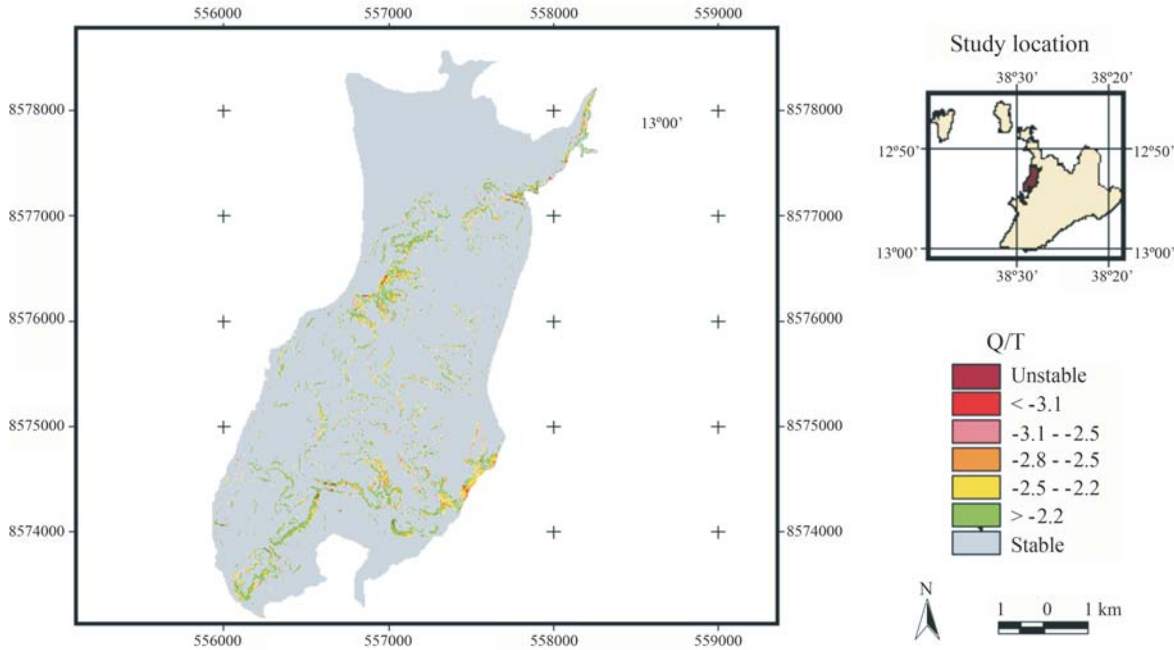

Figure 7 - Shallow landslide susceptibility map expressed by the ratio *Q/T* from the model that does not incorporate the spatial variability of soil properties.

gorithm simulation has identified less susceptible cells than the one that used the simple method. This behavior occurs due to the spatial variation of soil physical properties, and also because of the cohesion considered in the algorithm simulation. The latter decreases the slope instability since it makes the soil more cohesive and, consequently, decreases the percentage of unstable areas.

6. Conclusions

The mathematical modeling based on physical laws and GIS-based analysis constitutes a tool of great potential in identifying landslide susceptible areas by decreasing the subjectivity of the model and allowing for a rapid and efficient characterization over relatively large areas.

Regarding the simulations made to identify shallow landslide susceptible areas, it was observed that there was a high percentage for the class considered unconditionally stable in the study area, both in the simulation concerning the spatial variation of soil physical properties and in the simple method simulation.

It was also observed that there was an overestimate in the frequency potential for the unconditionally stable class in the simulation made by the algorithm in relation to the simple method.

Regarding the unconditionally unstable class, a slight difference between both simulations made was observed. The simulation in which there was spatial variation of soil physical properties presented a lower instability percentage. It happened because this simulation considered the influence of the cohesion in the landslide triggering.

Based on the results obtained, it was noticed that the SHALSTAB written in Avenue language was rather effec-

Table 4 - Frequency distributions of the susceptibility classes to shallow landslide in the Subúrbio Ferroviário de Salvador (Salvador, BA).

Stability classes	Log *Q/T* (algorithm)	Log *Q/T* (%)	Log *Q/T* (simple model)	Log *Q/T* (%)
Unstable	3959	0.04	4559	0.05
< -3.1	6287	0.07	5412	0.06
-3.1 - -2.8	7380	0.08	12403	0.13
-2.8 - -2.5	19412	0.21	51198	0.55
-2.5 - -2.2	55050	0.59	165057	1.78
> -2.2	185491	2.00	456142	4.93
Stable	8978884	97.00	8562166	92.49

tive and viable for using in planning cities of slope contention, besides being a user-friendly tool.

From the simulations made, it was observed that the result for the model, incorporating the soil physical properties, when compared to the results obtained with the simple method, has presented significant differences. It contributes to a more effective prediction in shallow landslide susceptible areas. This shows that better results may be obtained if the model is applied to areas where more data on relevant soil properties is available.

References

Augusto Filho, O. & Wolle, C.M. (1996) Landslide risk map: A methodological proposal and its application to the municipality of Ilhabela, SP. Solos e Rochas, v. 19:1, p. 45-62 (in Portuguese).

Barata, F.E. (1969) Landslides in the tropical region of Rio de Janeiro. Proc. 7th Int. Confer. on Soil Mech. and Found.Eng., Mexico. ISSMFE, London, pp. 507-516.

Beven, K.J. & Kirkby, M.J. (1979) A physically based, variable contributing area model of basin hydrology. Bulletin of Hydrological Sciences, v. 24:1, p. 43-69.

Brito, C.C.T. (1997) Lack of the urban land in Salvador and its consequences in the future reproduction of the urban space. Dissertação de Mestrado, Instituto de Geociências, Universidade Federal da Bahia, Salvador, 130 pp. (in Portuguese)

Carrara, A. (1983) A multivariate model for landslide hazard evaluation. Mathematical Geology. 15:3, p. 403-426.

Carrara, A.C.; Detti, R.; Guzzetti, F.; Pasqui, V. & Reichenbach, P. (1991) GIS techniques and statistical models in evaluating landslide hazard. Earth Surface Processes and Landforms, v. 16:5, p. 427-445.

Carson, M.A. & Kirkby, M.J. (1972) Hillslope Form and Process. Cambridge University Press, Cambridge, 475 pp.

Codesal (2002) Most serious accidents occurred by rains in Salvador between 1993 and 2002 - Relatório Técnico. 10 pp.

Cruz, O. (1974) Serra do Mar and Offshore in the Caraguatatuba-SP Area. Série Teses e Monografias, Instituto de Geografia, Universidade de São Paulo, São Paulo, 181 pp. (in Portuguese).

Dietrich, W E.; Bellugi, D. & Real de Asua, R. (2001) Validation of the shallow landslide model, SHALSTAB, for forest management. In: Wigmosta, M.S. & Burges, S.J. (eds), Land Use and Watersheds: Human Influence on Hydrology and Geomorphology in Urban and Forest Areas. Water Science and Application Monograph, Proc. American Geophysical Union, v. 2, p. 195-227.

Dietrich, W.E. & Montgomery, D.R. (1998) SHALSTAB: A digital terrain model for mapping shallow landslide potencial. National Council of the Paper Industry for Air and Stream Improvement (NCASI), Technical Report, 29 pp.

Dietrich, W.E.; Reiss, R.; Hsu, M.-L. & Montgomery, D.R. (1995) A process- based model for colluvium soil depth and shallow landsliding using digital elevation data. Hydrological Processes, v. 9, p. 383-400.

Dietrich, W.E.; Wilson, C.J.; Montgomery, D.R. & Mckean, J. (1993) Analysis of erosion thresholds, channel networks and landscape morphology using a digital terrain model. The Journal of Geology, v. 101, p. 259-278.

Dietrich, W.E.; Wilson, C.J.; Montgomery, D.R.; Mckean, J. & Bauer, R. (1992) Erosion thresholds and land surface-morphology. Geology, v. 20:8, p. 675-679.

Fernandes, N.F.; Guimarães, R.F.; Gomes, R.A.T.; Vieira, B.C.; Montgomery, D.R. & Greenberg, H. (2004) Topographic controls of landslides in Rio de Janeiro: field evidences and modeling. Catena, v. 55:2, p. 163-181.

Gao, J. (1993) Identification of topographic settings conducive to landsliding from DEM in Nelson County, VA, USA. Earth Surface Processes and Landforms, v. 18:7, p. 579- 591.

Geohidro (1993) Managing Plan of Draining and Stabilization of Soil Slopes in Salvador. Geohidro, Salvador, 233 p (in Portuguese).

Gomes, R.A.T.; Guimarães, R.F.; Carvalho Júnior, O.A. & Fernandes, N.F. (2005) Analysis of a landslides model prediction (Shalstab) in different cartographic scales. Revista Solos e Rochas, v. 28:1, p. 85-97 (in Portuguese).

Guimarães, R.F.; Montgomery, D.R.; Greenberg, H.M.; Fernandes, N.F.; Gomes, R.A.T. & Carvalho Júnior, O.A. (2003a) Parameterization of soil properties for a model of topographic controls on shallow landsliding: Application to Rio de Janeiro. Engineering Geology, v. 69:1-2, p. 99-108.

Guimarães, R.F.; Fernandes, N.F.; Gomes, R.A. T. & Carvalho Júnior, O.A. (2003b) Theoretical reviews of landslides model prediction shallow stability (Shalstab). Espaço & Geografia, v.6:2, p.133-150 (in Portuguese).

Hutchinson, M.F. (1989) A new procedure for gridding elevation and stream linedata with automatic removal of spurious pits. Journal of Hydrology, v. 106, p. 211-232.

Iverson, R.M. (2000) Landslide triggering by rain infiltration. Water Resources Research, v. 36:7, p. 1897-1910.

Lacerda, W.A. (1997) Stability of natural slopes along the tropical coast of Brazil. Proc. Symp. Recent Developments in Soil and Pavement Mechanics, A.A. Balkema, Rotterdam, pp. 17-39.

Larsen, M.C. & Torres-Sanchez, A.J. (1998) The frequency and distribution of recent landslides in three montane tropical regions of Puerto Rico. Geomorphology, v. 24:4, p. 309-331.

Macdonald, D.; Gomez-Perez, I.; Franzese, J.; Spalletti, L.; Lawver, L.; Gahagan, L.; Dalziel, I.; Thomas, C.; Trewin, N.; Hole, M. & Paton, D. (2003) Mesozoic break-up of SW Gondwana: implications for regional hydrocarbon potential of the southern South Atlantic. Marine and Petroleum Geology, v. 20:3-4, p. 287-308.

Magalhães, M.A.C. (1993) Mass Movement and Soil Occupation in Engenho Velho da Federação Neighbor. Salvador - Bahia. Dissertação de Mestrado, Instituto de Geociências, Universidade Federal da Bahia, Salvador, 129 pp. (in Portuguese)

Menezes, V.G. (1987) The rainfall and landslides in hillslopes in the Recife urban area. Proc. 50 Congresso Brasileiro de Geologia de Engenharia, São Paulo, v. 2, p. 347-358.

Moeyersons, J. (2003) The topographic thresholds of hillslope incisions in southwestern Rwanda. Catena, v. 50:2-4, p. 381-400 (in Portuguese).

Montgomery, D.R. & Dietrich, W.E. (1994) A physically based model for the topographic control on shallow landsliding. Water Resources Research, v. 30:4, p. 1153-1171.

Montgomery, D.R.; Sullivan, K. & Greenberg, M.H. (1998) Regional test of a model for shallow landsliding. Hydrological Processes, v. 12:6, p. 943-955.

Montgomery, D.R.; Wright, R.H. & Booth, T. (1991) Debris flow hazard mitigation for colluvium-filled swales. Bulletin Association Engineering Geology, v. 28, p. 303-323.

Moore, I.D.; O'Loughlin, E.M. & Burch, G.J. (1988) A counter-based topographic model for hydrological and ecological applications. Earth Surface and Processes and Landforms, v. 13, p. 305-320.

Okimura, T. & Ichikawa, R. (1985) A prediction method for surface failures by movements of infiltrated water in a surface soil layer. Natural Disaster Science, 7:1, p. 41-51.

O'Loughlin, E.M. (1986) Prediction of surface saturation zones in natural catchments by topographic analysis. Water Resources Research, 22:5, p. 794-804.

Pack, R.T.; Tarboton, D.G. & Goodwin, C.N. (1998) Terrain stability mapping with SINMAP, technical description and users guide for version 1.00. Report Number 4114-0, Terratech Consulting Ltd., Salmon Arm, Canada, 68 pp.

Paim, J.S.; Costa, M.C.N.; Mascarenhas, J.C.S. & Silva, L.M.V. (1999) The distribution of violence: mortality due to external causes in Salvador, Brazil. Revista Panamericana de Salud Publica, v. 6:5, p. 321-332.

Peixoto, C.S. (1968) The Physics Factors Conditioning the Problems in Salvador City. Tese de Doutorado, Faculdade de Filosofia, Universidade Federal da Bahia, Salvador, 186 pp (in Portuguese).

Ploey, J. & Cruz, O. (1979) Landslides in the Serra do Mar, Brazil. Catena, v. 6:2, p. 111-122.

Rossetti, D.F. & Góes, A.M. (2001) Imagine upper Tertiary to Quaternary deposits from northern Brazil applying ground penetrating radar. Revista Brasileira de Geociências, v. 31:2, p. 195-202.

Santos, S.M.; Barcellos C. & Carvalho M.S. (2006) Ecological analysis of the distribution and socio-spatial context of homicides in Porto Alegre, Brazil. Health & Place, v. 12:1, p. 38-47.

Serpa, A. & Garcia, A. (1999) The tourist potential of the subúrbio ferroviário de Salvador from inhabitants' point of view. Lima, L.C. (ed) Da Cidade ao Campo: A Diversidade do Saber - Fazer Turístico. FUNECE/UEC, Fortaleza, pp. 237-246 (in Portuguese).

Smyth, C.G. & Royle, S.A. (2000) Urban landslide hazards: incidence and causative factors in Niterói, Rio de Janeiro State, Brazil. Applied Geography, v. 20:2, p. 95-118.

Terlien, M.T.J. (1997) Hydrological landslide triggering in ash-covered slopes of Manizales (Columbia). Geomorphology, v. 20:1-2, p. 165-175.

Tricart, J. & Silva, T.C. (1968) Studies on Geomorphology in Bahia and Sergipe. Fundação de Desenvolvimento Científico da Bahia Press, Salvador, 189 pp. (in Portuguese).

Van Asch, T.; Kuipers, B. & Van Der Zanden, D.J. (1993) An information system for large scale quantitative hazard analyses of landslide. Zeitschrift für Geomorphologie, v. 87, p. 133-140.

Viana, C.F.; Gama Junior, E.G.; Simões, I.A.; Moura, J.A.; Fonseca, J.R. & Alves, R.J. (1971) Stratigraphic review in the Recôncavo/Tucano basin. Boletim Técnico Petrobrás, 14:3-4, p. 157-192 (in Portuguese).

Wacquant, L. & Wilson, W.J. (1989) The cost of racial and class exclusion in the inner city. Annals of the American Academy of Political and Social Science, v. 50:1, p. 8-25.

Wu, W. & Sidle, R.C. (1995) A distributed slope stability model for steep forested basins. Water Resources Research, 31:8, p. 2097-2110.

Zhou, C.H.; Lee, C.F.; Li, J. & Xu, Z.W. (2002) On the spatial relationship between landslides and causative factors on Lantau Island, Hong Kong. Geomorphology, v. 43:3-4, p. 197-207.

The Influence of the Foundation Settlements on the Column Loads of a Building

Juliane Cristina Gonçalves, Paulo Eduardo Lima de Santa Maria,
Fernando Artur Brasil Danziger, Eliane Maria Lopes Carvalho

Abstract. The loads on columns related to foundation settlements of a building localized in the city of Rio de Janeiro have been analysed. Settlements and strains in some columns have been measured from the beginning of construction. The structural behaviour was simulated with the finite element method with a model for each building stage related to the measurements. The loads evaluated considering no foundation settlements have been compared to the loads obtained with the measured settlements as prescribed displacements. The loadings thus obtained were also compared to those estimated by the columns strains.

Key words: foundation, soil-structure interaction, settlement measurement, strain measurement.

1. Introduction

The design of the structure and the foundation of a building are generally independently performed (*e.g.* Gusmão, 1990). Therefore, the soil-structure interaction is not considered. In general, there is a load transfer from the columns that have the trend to have higher settlements to those with smaller settlements. Thus there is a trend of uniformization of the settlements. This subject has been studied by a number of researchers, *e.g.* Meyerhof (1953), Chamecki (1954), Goschy (1978), Gusmão (1990), Gusmão and Gusmão Filho (1994a, 1994b), Gusmão Filho (1998), Moura (1995), Aoki (1997), Danziger *et al*. (1997), Santa Maria *et al*. (1999) and Soares (2004).

The present paper analyses the column loads of a building considering two situations. In the first one the foundations are assumed to have no settlements, which is the usual assumption in the design of a structure. The second one takes into account the settlements that have been measured from the beginning of construction. In both cases the structure was analysed with the use of the finite element method. The analysed models correspond to each available set of measurements.

Since the strains in columns have also been measured from the beginning of construction, a comparison between the loads estimated from the strains and from the finite element analysis is also made.

The analysed building is one out of nine instrumented buildings included in a research cooperation among COPPE/UFRJ, UFF and building contractor Construtora Ben.

2. The Building

2.1. General characteristics

The analysed building, designated SFA, is situated in Recreio dos Bandeirantes, west zone of the Rio de Janeiro city, and it is typical from this huge area where the city of Rio de Janeiro is growing towards. It is a reinforced concrete building, with one access floor, two similar floors, the penthouse, as well as an elevated water tank. Verandas in cantilever are present in the front of the building (Fig. 1).

There are 21 columns arriving at the ground level, and design loads vary from 220 kN to 1960 kN. Footings have been used, installed at a depth 1.5 m below the ground level. An average allowable soil stress of 200 kPa was

Figure 1 - View of SFA building.

Juliane Cristina Gonçalves, PhD. Student, COPPE, Universidade Federal do Rio de Janeiro, Rio de Janeiro, RJ, Brazil. e-mail: juliane@acessa.com.
Paulo Eduardo Lima de Santa Maria, Associate Professor, COPPE/Escola Politécnica, Universidade Federal do Rio de Janeiro, Rio de Janeiro, RJ, Brazil. e-mail: paulosm@coc.ufrj.br.
Fernando Artur Brasil Danziger, Associate Professor, COPPE/Escola Politécnica, Universidade Federal do Rio de Janeiro, Rio de Janeiro, RJ, Brazil. e-mail: danziger@coc.ufrj.br.
Eliane Maria Lopes Carvalho, Associate Professor, Universidade Federal Fluminense, Niterói, RJ, Brazil. e-mail: elianemaria@vm.uff.br.
Submitted on May 23, 2007; Final Acceptance on July 4, 2007; Discussion open until April 30, 2008.

adopted. Fig. 2 shows a plan with the columns location and loads.

2.2. Soil characteristics

Standard penetration tests (SPT's) have been the only soil test used to characterize the soil, and the obtained profiles are presented in Fig. 3. Fine to medium sand, from loose to dense, mostly grey but in some layers brown, is found from the ground surface to 20 m depth. Organic clay layers, grey, soft and medium, as well as a hard silty clay layer are found interbedded with sand layers in the range 20 m - 26 m depth. The characteristics of those sand layers are similar to the layers found in the upper part of the profile.

3. Settlements and Strains Measurements

3.1. Procedure used to measure the settlements

Settlements have been measured from March 1993 until February 1996. Corrosion-free seats have been installed in some columns, at a height of around 1 m above the ground level.

Due to the high cost to install a bench-mark, corrosion-free seats have been installed outside the building, in places where the influence of the building is assumed to be negligible. Optical leveling has been used to evaluate the settlements. In every set of measurements the obtained values have been checked against different external reference values. Other details, both from the procedure and the equipment used, can be found in Danziger *et al*. (1995, 1997, 2000) and Gonçalves (2004).

3.2. Procedure used to measure the strains

Strains have been measured in a shorter period than the settlements, from March 1993 until January 1994. The experience associated with the procedure used comes from the 1970's, when Soares (1978) and Soares and Carim (1978) used it to evaluate the strut loads in the Rio de Janeiro Subway. Two pins, 250 mm vertically apart, have been installed in the middle section of the columns. Dents have been punched in the pins, in order to provide the "perfect" suitable fitting for a mechanical extensometer. The Huggenberg extensometer, which consists of an internal rod moving inside a tube coupled with an extensometer able to measure 0.001 mm, has been used (Fig. 4). The extensometer measures the length variation between the 2 reference pins. From this measurement, the strain values are obtained. Values of strain have been obtained in the four faces of columns C11 and C17, as well as in two parallel faces of columns C10 and C15. Further details can be obtained in Gonçalves (2004).

4. The Evaluation of Column Loads from the Strain Values

The strain values have been measured aiming at the evaluation of the column loads in different stages of the

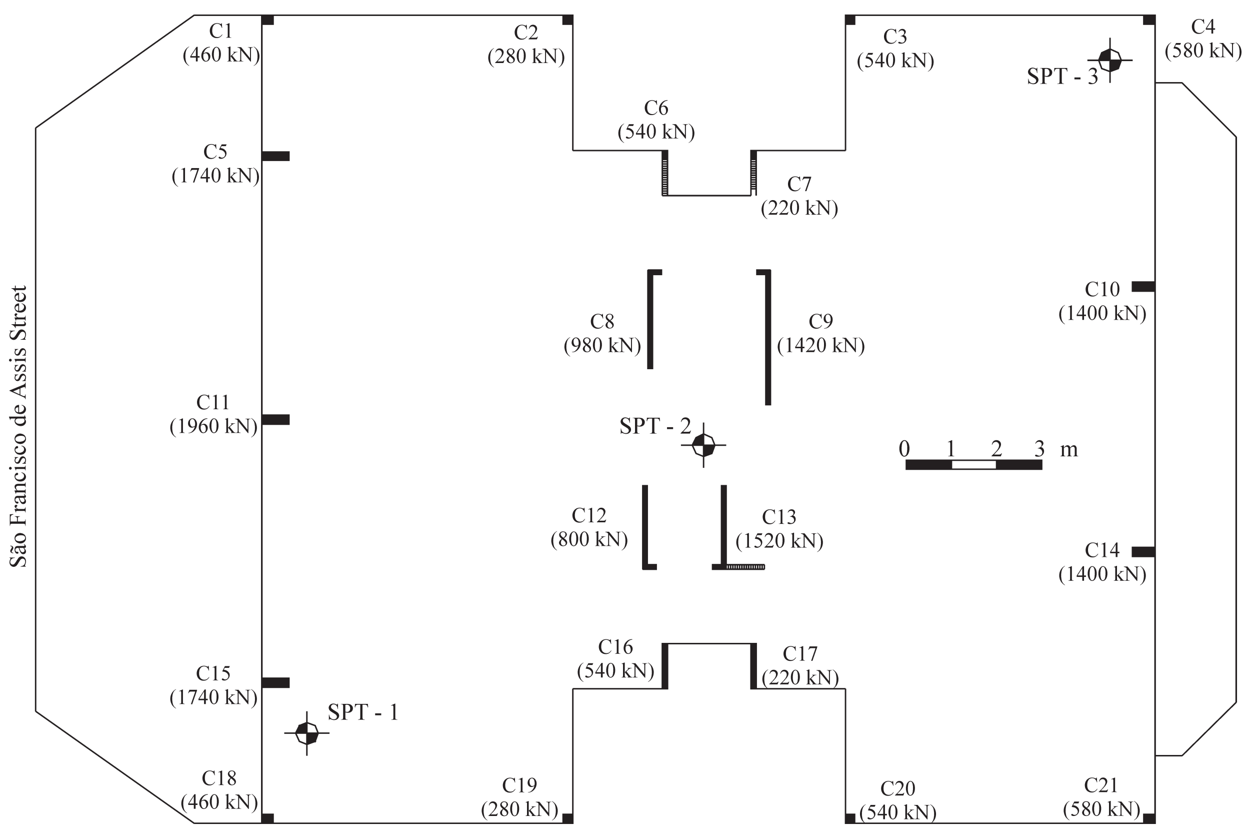

Figure 2 - Location of columns and SPT's performed (Gonçalves *et al*., 2004).

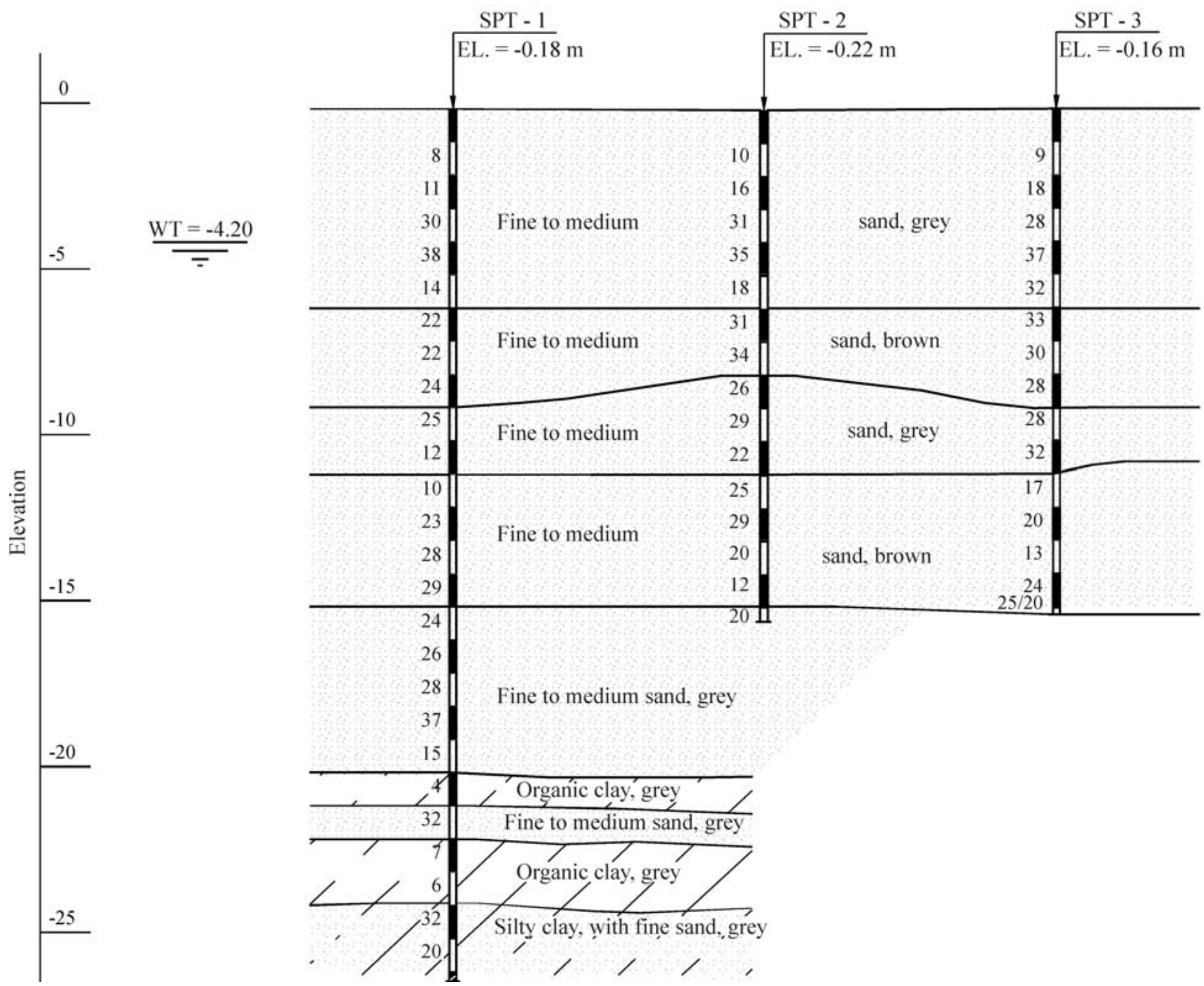

Figure 3 - Soil profile.

building construction. However, such evaluation is not straightforward, since the strains are influenced not only by the column loads, but also by concrete creep, shrinkage and thermal strain. Such values must therefore be estimated.

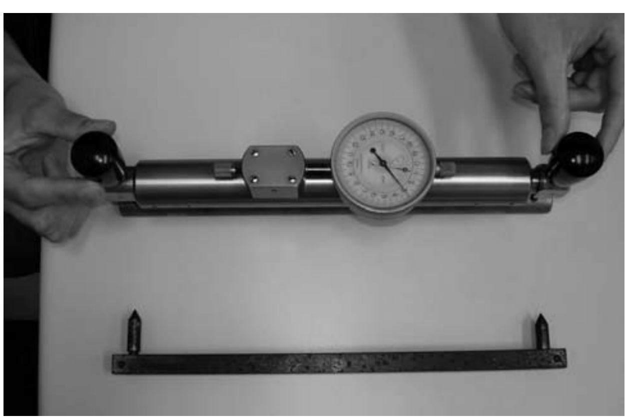

Figure 4 - Mechanical extensometer Huggenberg used to measure the strains in the columns.

According to the CEB-FIP Model Code (1990), the total strain at time t, $\varepsilon_c(t)$, of a concrete member, uniaxially loaded at time t_0 with a constant stress $\sigma_c(t_0)$, may be expressed as

$$\varepsilon_c(t) = \varepsilon_{ci}(t_0) + \varepsilon_{cc}(t) + \varepsilon_{cs}(t) + \varepsilon_{cT}(t) \quad (1)$$

or

$$\varepsilon_c(t) = \varepsilon_{c\sigma}(t) + \varepsilon_{cn}(t) \quad (2)$$

where $\varepsilon_{ci}(t_0)$ = initial strain at loading; $\varepsilon_{cc}(t)$ = creep strain at time $t > t_0$; $\varepsilon_{cs}(t)$ = shrinkage strain; $\varepsilon_{cT}(t)$ = thermal strain; $\varepsilon_{c\sigma}(t) = \varepsilon_{ci}(t) + \varepsilon_{cc}(t)$, stress dependent strain; $\varepsilon_{cn}(t) = \varepsilon_{cs}(t) + \varepsilon_{cT}(t)$, stress independent strain.

For stresses and strains varying with time, assuming the validity of the superposition principle, one can obtain

$$\varepsilon_c(t) = \sigma_c(t_0) J(t, t_0) + \int_{t_0}^{t} J(t, \tau) \frac{\partial \sigma_c(\tau)}{\partial \tau} d\tau + \varepsilon_{cn}(t) \quad (3)$$

where $\sigma_c(t_0)$ = initial stress; $J(t, \tau)$ = creep function or creep compliance: $J(t,\tau)=\left[\frac{1}{E(\tau)}+\frac{\phi(t,\tau)}{E_{ci}}\right]$; $E(\tau)$ = modulus of elasticity of the concrete at the time of application of the load increase; τ = dummy time variable; $\phi(t, \tau)$ = creep coefficient; E_{ci} = modulus of elasticity of the concrete at the age of 28 days; $\frac{\partial\sigma_c(\tau)}{\partial\tau}d\tau$ = infinitesimal increment of stress.

4.1. Estimating the concrete creep, shrinkage and thermal strain according to the CEB-FIP Model Code (1990)

The equations used to estimate the concrete creep, shrinkage and thermal strain, according to the CEB-FIP Model Code (1990), are valid for concrete structures (12 MPa < f_{ck} ≤ 80 MPa) subjected to a compression stress $|\sigma_c| < 0.4 f_{cm}(t_0)$ at age of loading t_0 and exposed to mean relative humidity between 40 and 100% and mean temperature between 5 and 30 °C, where f_{ck} = characteristic compressive strength of concrete; f_{cm} = mean compressive strength of concrete at the age of 28 days.

The thermal strain has not been considered in the analysis because the concrete temperature was not measured. It is believed that this strain has not been significant with respect to the others, due to the geometric configuration of the columns in the building. Russo Neto (2005), in a similar analysis for a precast concrete structure with precast concrete piles in the city of Curitiba, did obtain a significant influence of the temperature on the measured strain values. However, the geometric positioning of the columns in this building was rather different from the one analysed in the present paper. Moreover, the column cross-section of the Russo Neto (2005) building was different from the ones analysed herein.

4.1.1. Concrete creep

The creep coefficient can be estimated from Eq. (4),

$$\phi(t,\tau)=\phi_0\,\beta_c\,(t-\tau) \tag{4}$$

where ϕ_0 = notional creep coefficient, depending on the relative humidity of the ambient environment, on the section homogenized, on its perimeter, and on the mean compressive concrete strength at the age of 28 days; $\beta_c(t - \tau)$ = coefficient describing the development of creep with time after loading; t = concrete age (days) at the moment considered; τ = concrete age (days) at loading.

The CEB-FIP Model Code (1990) presents the equations necessary to estimate ϕ_0 and $\beta_c(t - \tau)$.

The creep strain occurring in a reinforced concrete member is smaller than the one in a concrete member, since in a reinforced concrete member there is a load transfer from the concrete to the steel throughout the time. Because of that, the concrete strain in the present analysis was corrected according to an analysis carried out by Santa Maria (1997), since the homogenized area had been used in the calculations.

4.1.2. Concrete shrinkage

The strain due to shrinkage can be estimated from Eq. (5)

$$\varepsilon_{cs}(t,t_s)=\varepsilon_{cso}\beta_s(t-t_s) \tag{5}$$

where ε_{cso} = notional shrinkage coefficient, depending on the type of cement, the mean compressive concrete strength at the age of 28 days, and on the relative humidity of the ambient environment; $\beta_s(t - t_s)$ = coefficient describing the development of shrinkage with time; t = concrete age (days) at the time considered; t_s = concrete age (days) at the beginning of shrinkage.

The CEB-FIP Model Code (1990) presents the equations necessary to estimate ε_{cso} and $\beta_s(t - t_s)$.

5. Soil-Structure Interaction

5.1. Numerical model of the building structure

Five 3D finite element models of the framed structure, presented in Figs. 5 to 7, have been developed, corresponding to each available series of settlement and strain measurements (named stages), as shown in Table 1. Figure 7 represents the 3 last series of measurements (stages), for which the differences are related to the applied loads after the completion of the concrete structure.

Frame elements have been used to discretize beams and columns. However, the central wall-columns C8, C9, C12 and C13 have been simulated as shell elements due to their high stiffness. Shell elements have also been used to discretize the slabs. An elastic behaviour was assumed for

Figure 5 - Numerical model corresponding to 1st stage (Gonçalves, 2004).

Figure 6 - Numerical model corresponding to 2nd stage (Gonçalves, 2004).

Figure 7 - Numerical model corresponding to 3rd, 4th and 5th stages (Gonçalves, 2004).

the whole structure. All analyses have been performed with the program SAP 2000 (1996).

5.2. Column loads in different hypotheses

The column loads have been estimated for two situations regarding the foundation settlements. In the first one the foundations are assumed to present no settlements, which is the usual assumption in the design of a structure. The second one takes into account the settlements that have been measured from the beginning of construction. Once the measurement of settlements have not been performed in all columns, settlement values have been adopted considering the symmetry observed in the structure with respect to an axis at right angle to the street. Moreover, the soil has been assumed constituted by homogeneous layers. Measured and adopted settlement values are included in Table 2.

Table 1 - Numerical models and building stages (Gonçalves, 2004).

Model	Date*	Building stage
1st stage	17/5/1993	1st floor structure concreted without the front cantilevers
2nd stage	17/8/1993	2nd floor structure concreted
3rd stage	26/1/1994	Structure and brick walls concluded
4th stage	3/8/1995	Whole structure
5th stage	7/2/1996	Building in use

*Reference (zero) readings taken in 31/3/1993.

6. Analysis of the Results

6.1. Comparison of column loads obtained for the hypotheses of no settlements and measured settlements

The column loads obtained from the finite element analysis with the no settlements hypothesis are presented in Table 3, for each construction stage. The ratio between the loads obtained for the 5th stage and the design loads is also included in the table. The design loads have been obtained by calculating separately slabs, beams and columns, disregarding the actual interaction among these members. The lower part of the table contains the ratio of load (in percentage) in each stage with respect to the 5th stage.

The ratio total load (including the loads of all columns) of 5th stage and the design load is 89%, *i.e.* did not reach 100%. Minor simplifications in the model (the non-consideration of the water load in the elevated water tank, as well as the load of the elevators machinery) do not justify such difference.

The last column of Table 3 presents the difference (in percentage), for each column, between the ratio 5th stage load/design load and 0.89, the average ratio for all columns. It can be observed that the differences have been quite significant. In fact, a value as high as 30% was obtained, which was attributed to the non conventional building structure. Thus, this kind of structure suggests the need for using of more refined design methods (like e.g. the finite element method) than the commonly used. High differences between design loads obtained from the usual method and the loads obtained by the finite element method (in the range +58% to -45%) have been obtained by Costa (2003) for a similar structure.

The influence of the settlements on the column loads is illustrated in the comparison included in Table 4. The column loads in Table 4 have been obtained in both hypotheses (no settlements and measured settlements) from the analyses performed with the finite element method. The differences between the column loads for both hypotheses (in percentage), which can be considered an indication of

Table 2 - Measured and adopted settlement values (Gonçalves, 2004).

Column	Settlement (mm)				
	1st stage 17/5/1993	2nd stage 17/8/1993	3rd stage 26/1/1994	4th stage 3/8/1995	5th stage 7/2/1996
C1	0.36*	1.02*	1.94	3.23*	5.10*
C2	0.45	1.08	2.05	3.49	4.89
C3	0.58*	1.27*	2.41	4.58*	6.41
C4	0.65	1.72	3.00	6.63	7.65
C5	0.73	1.71	2.96	4.41	6.43
C6	0.50	1.20	2.28	3.88	5.00
C7	0.38	0.91	1.73	2.94	3.75
C8	0.72*	1.59*	3.03*	5.26*	7.21
C9	0.48*	1.40*	3.12*	5.21*	7.14
C10	0.98*	2.32*	3.67*	6.02*	7.56*
C11	0.73*	1.75*	3.12*	4.94*	6.95*
C12	0.56*	1.21*	2.64*	4.60	7.21
C13	0.48	1.40	3.12	5.21	7.14
C14	0.98	2.32	3.67	6.02	7.56
C15	0.73*	1.71*	2.96*	4.41*	6.43*
C16	0.50	1.20	2.28	3.88	5.00
C17	0.38	0.91	1.73	2.94	3.75
C18	0.36	1.02	1.94	3.23	5.10
C19	0.45	1.08	2.05	3.49	4.89
C20	0.58	1.27	2.41	4.58	6.41
C21	0.65*	1.72*	3.00*	6.63*	7.65*

*Measured values.

the soil-structure interaction, are also included in the table. The averages of such differences are shown in the lower part of the table.

Figures 8 and 9 present the mentioned difference as a function of time, where the date of reference (zero) readings (31st March 1993) has been considered as time equal to 0. Figure 8 contains the columns that presented a load increase, and Fig. 9 a load decrease at least for some period, with respect to the no settlement hypothesis. It is worth emphasizing that since the structure has been modelled as an elastic structure, time is only associated with load variation.

From Table 4 and Figs. 8 and 9 it can be observed that 11 columns have presented small load differences (smaller than 5%) with respect to the no settlements hypothesis. These are C2, C3, C4, C5, C10, C11, C14, C15, C19, C20 and C21. The columns C2, C3, C4, C5 and C10 are symmetrically located with regard to columns C19, C20, C21, C15 and C14, respectively. The columns C5, C11 and C15 are located in the frontal part of the building, very much influenced by the cantilever (5 m), and have the highest design loads: C5 and C15, 1740 kN, and C11, 1960 kN. All these columns, despite of the particular situation of C5, C11 and C15 are peripheral columns.

The column C13 could have been included in the same previous situation (with respect to the no settlements hypothesis smaller than 5%), except for the 2nd stage, where a difference of 9% was obtained. This value is discussed afterwards.

The other columns have presented higher differences with respect to the no settlement hypothesis. The columns C1 and C18, which are symmetrically located in the frontal part of the building (at the corners), have always shown differences higher than 5% (C1 higher than 10%), as it would be expected. In fact, it is usual a load transfer from the internal columns to the external columns, or in other words, a load increase in the external columns and a load decrease in the internal columns with respect to the no settlements hypothesis.

The columns C8, C9 and C12 have shown a load increase with respect to the no settlement hypothesis, differently from the expected behaviour. Besides, all those columns have shown a trend of an increase of the soil-structure interaction with time. It is worth mentioning that settle-

Table 3 - Column loads for the hypothesis of no foundation settlements (Gonçalves, 2004).

Column	Design load (kN)	1st stage (kN)	2nd stage (kN)	3rd stage (kN)	4th stage (kN)	5th stage (kN)	Load 5th stage/ Design load	Difference* with respect to 89%
C1	460	19	50	189	253	274	0.60	0.29
C2	280	30	38	161	203	212	0.76	0.13
C3	540	53	97	346	445	501	0.93	-0.04
C4	580	52	89	304	384	432	0.74	0.15
C5	1740	110	407	1089	1441	1672	0.96	-0.07
C6	540	55	87	304	390	438	0.81	0.08
C7	220	19	42	172	219	244	1.11	-0.22
C8	980	108	166	554	708	816	0.83	0.06
C9	1420	139	254	771	963	1137	0.80	0.09
C10	1400	166	322	817	1025	1221	0.87	0.02
C11	1960	158	504	1372	1861	2169	1.11	-0.22
C12	800	92	161	489	628	717	0.90	-0.01
C13	1520	110	178	865	1103	1275	0.84	0.05
C14	1400	164	319	799	1006	1199	0.86	0.03
C15	1740	122	415	1081	1459	1686	0.97	-0.08
C16	540	79	113	343	446	498	0.92	-0.03
C17	220	25	41	195	235	262	1.19	-0.30
C18	460	19	53	200	270	293	0.64	0.25
C19	280	32	40	169	219	230	0.82	0.07
C20	540	44	88	330	427	481	0.89	0.00
C21	580	52	90	307	390	439	0.76	0.13
Σ	18200	1648	3554	10857	14075	16196	average	0.89
Percentage with respect to the 5th stage		10	22	67	87	100		

*The negative sign indicates that the value corresponding to the 5th stage was greater than 89% of the design load.

ments have not been measured in the column C12, which is the one presenting the highest load increase, especially for the 4th and 5th stages. The adopted settlement values may have been overestimated, since they have been obtained from the increase rate of settlements of column C8, due to its similarity with C12.

The columns C6, C7, C16 and C17 have shown load decrease with time with respect to the no settlement hypothesis, and this trend increased with time, also depicting the soil-structure interaction influence with time.

It can be observed that in the inner part of the building the columns C6, C7, C8, C9 C12, C16 and C17 have been the most affected by the structure stiffness increasing with time.

This behaviour has been attributed to the particular characteristics of the structure, which has different floors, central columns with high stiffness and, especially, large cantilevers (5 m) corresponding to the veranda, which have produced higher loads in the frontal columns, mainly C5, C11 and C15, than the internal loads, differently from regular buildings, where higher loads are found in the central columns.

Some columns (C1, C2, C6, C8, C12, C13, C16, C18 and C19) have presented a significant variation of their behaviour in the 2nd measurement with respect to the other series of measurements. This is probably related to a special construction aspect, the removal of the shoring of the cantilever slab from the first to the second stages.

It was also found that the load redistribution throughout the time, which can be represented by the average of load redistributions of all columns, was small (3%) only in the first series of measurements (see Table 4). In the others stages, this value was about 7%. In other words, the first series of measurements would be the only one showing a stiffness smaller than the others.

It is worth emphasizing that the differences of column loads for the two structural models analysed (the procedure disregarding the interaction among the structural members and the finite element method) were higher than the load differences obtained when the hypotheses of no settlements

Table 4 - Column loads for two hypotheses: no settlements and measured settlements (Gonçalves, 2004).

Column	Design load (kN)	1st stage (kN) settlements meas. no Difference	2nd stage (kN) settlements meas. no Difference	3rd stage (kN) settlements meas. no Difference	4th stage (kN) settlements meas. no Difference	5th stage (kN) settlements meas. no Difference
C1*	460	21-19	62-50	213-189	279-253	303-274
		11%	24%	13%	10%	11%
C2	280	30-30	39-38	163-161	207-203	216-212
		0%	3%	1%	2%	2%
C3*	540	52-53	96-97	341-346	435-445	477-501
		-2%	-1%	-1%	-2%	-5%
C4	580	52-52	91-89	308-304	380-384	435-432
		0%	2%	1%	-1%	1%
C5	1740	107-110	391-407	1054-1089	1407-1441	1630-1672
		-3%	-4%	-3%	-2%	-3%
C6	540	53-55	78-87	274-304	338-390	374-438
		-4%	-10%	-10%	-13%	-15%
C7	220	17-19	37-42	153-172	191-219	214-244
		-11%	-12%	-11%	-13%	-12%
C8*	980	110-108	177-166	590-554	765-708	895-816
		2%	7%	6%	8%	10%
C9*	1420	142-139	267-254	818-771	1045-963	1237-1137
		2%	5%	6%	9%	9%
C10*	1400	165-166	317-322	805-817	1015-1025	1204-1221
		-1%	-2%	-1%	-1%	-1%
C11*	1960	158-158	503-504	1362-1372	1828-1861	2129-2169
		0%	0%	-1%	-2%	-2%
C12*	800	100-92	193-161	587-489	787-628	919-717
		9%	20%	20%	25%	28%
C13	1520	106-110	162-178	840-865	1067-1103	1223-1275
		-4%	-9%	-3%	-3%	-4%
C14	1400	164-164	315-319	788-799	995-1006	1182-1199
		0%	-1%	-1%	-1%	-1%
C15*	1740	120-122	403-415	1055-1081	1434-1459	1654-1686
		-2%	-3%	-2%	-2%	-2%
C16	540	75-79	97-113	301-343	372-446	409-498
		-5%	-14%	-12%	-17%	-18%
C17	220	25-25	40-41	168-195	193-235	215-262
		0%	-2%	-14%	-18%	-18%
C18	460	20-19	61-53	218-200	288-270	314-293
		5%	15%	9%	7%	7%
C19	280	32-32	42-40	173-169	226-219	238-230
		0%	5%	2%	3%	3%
C20	540	43-44	88-88	328-330	423-427	467-481
		-2%	0%	-1%	-1%	-3%
C21*	580	52-52	91-90	310-307	386-390	439-439
		0%	1%	1%	-1%	0%
Average**		3%	7%	6%	7%	7%

*Columns with settlement measurement; **Average of absolute values.

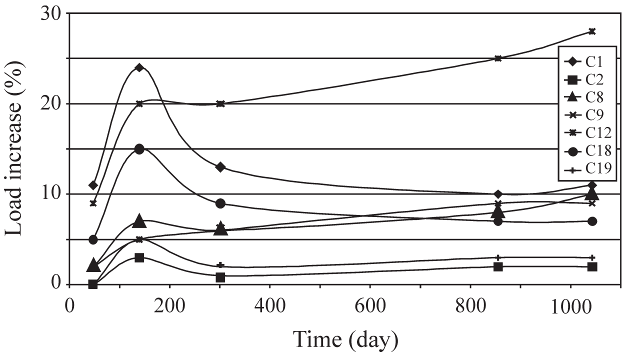

Figure 8 - Columns with load increase (%) with time.

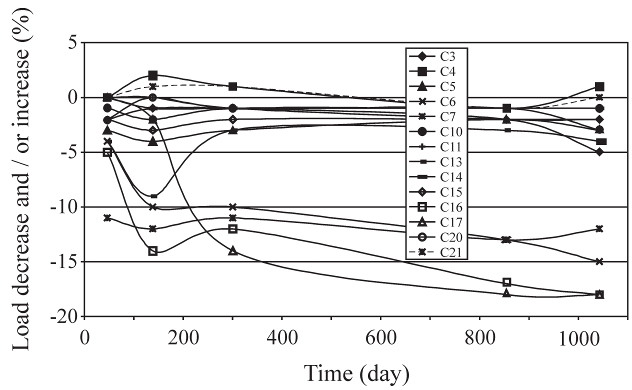

Figure 9 - Columns with load decrease (%), at least during a period, with time.

and measured settlements have been compared, but the same structural model (the finite element model) was used. This has been attributed to the particular features of the building, as previously mentioned, and also to the small measured settlements used in the analysis.

6.2. Comparison of the loads estimated from the strain measurements with the ones obtained from the finite element analysis

The average values of strain measured on the column faces are included in Table 5. The loads obtained from the strain values (*N*), taking into account the strains due to creep and shrinkage, as previously shown, are compared with the loads obtained from the finite element analysis, considering the structure subjected to the measured settlements (*Nprog*), in Table 6 and Fig. 10. The ratio between those values is also included in the table.

From both Table 6 and Fig. 10 one can observe that a good agreement between the loads is obtained only in the first stage of column C10. A trend of higher *N* values than

Table 5 - Strains measured (Gonçalves, 2004).

Dates	Days	Average strain			
		C10	C11	C15	C17
31/3/93 to 17/5/93	47	1.60 E -04	1.06 E -04	1.58 E -04	8.10 E -05
31/3/93 to 17/8/93	139	2.87 E -04	2.48 E -04	2.85 E -04	8.50 E -05
31/3/93 to 26/1/94	301	2.87 E -04	-	3.26 E -04	1.77 E -04

Table 6 - Column loads as obtained from the measured strain values (*N*) and from the finite element analysis (*Nprog*) (Gonçalves, 2004).

C10			
Model	*N* (kN)	*Nprog* (kN)	*N/Nprog*
1st stage	168	165	1.02
2nd stage	254	317	0.80
3rd stage	218	805	0.27
C11			
Model	*N* (kN)	*Nprog* (kN)	*N/Nprog*
1st stage	130	158	0.82
2nd stage	344	503	0.68
C15			
Model	*N* (kN)	*Nprog* (kN)	*N/Nprog*
1st stage	196	120	1.63
2nd stage	319	403	0.79
3rd stage	318	1055	0.30
C17			
Model	*N* (kN)	*Nprog* (kN)	*N/Nprog*
1st stage	49	25	1.96
2nd stage	-	40	-
3rd stage	-	168	-

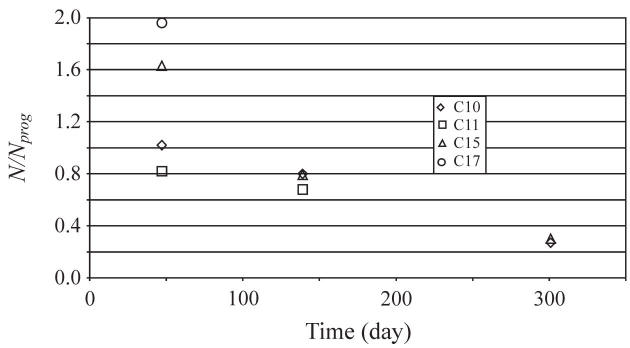

Figure 10 - Ratio between the column loads obtained from the measured strains and the loads from the finite element analysis versus time (Gonçalves, 2004).

Nprog values was obtained in the first stage while the opposite was found as time progresses.

For the second and third stages, although *Nprog* could have been overestimated by the finite element analysis, it is believed that the strain due to concrete shrinkage (or even the concrete creep) has been overestimated.

It was not possible to estimate the *N* values for the 2nd and 3rd stages in the case of C17, since the estimation of the strain due to concrete shrinkage was higher than the measured strain. This was due to the shape and perimeter of the column section (12 cm x 110 cm), which is very different from the other columns (C10, 20 cm x 50 cm, C15, 20 cm x 60 cm, C11, 20 cm x 70 cm), resulting in the estimation of high values of the strain due to shrinkage.

7. Conclusions

• The differences of column loads of the finite element analysis and the design loads have reached 30%, which was attributed to the non conventional building structure. Thus, this kind of structure suggests the need of use of more refined design methods (like *e.g.* the finite element method) than the commonly used to design building structures.

• The soil-structure interaction has been evaluated comparing two hypotheses: (i) no foundation settlements and (ii) measured settlements as input for the finite element analysis of the models developed. Eleven columns have shown differences between both hypotheses less than 5%. Some columns have shown differences higher than 5% differently from what it would be expected, the usual load transfer from the internal columns to the external columns, or in other words, a load increase in the external columns and a load decrease in the internal columns with respect to the no settlements hypothesis. This behaviour has been attributed to the particular characteristics of the structure, which has different floors, central columns with high stiffness and, especially, large cantilevers (5 m) corresponding to the veranda, which have produced higher loads in the frontal columns, especially C5, C11 and C15, than the internal loads, differently from regular buildings, where higher loads are found in the central columns.

• Some columns (C1, C2, C6, C8, C12, C13, C16, C18 and C19) have presented a significant variation of their behaviour in the 2nd stage with respect to the other stages. This has been attributed to a special construction aspect, the removal of the shoring of the cantilever slab from the first to the second stages.

• It was found that the load redistribution throughout the time, which can be represented by the average of load redistributions of all columns, was small (3%) only in the first stage. In the others stages, this value was about 7%. In other words, the first stage would be the only one showing a stiffness smaller than the others.

• The differences of column loads for the two structural models analysed (the procedure disregarding the interaction among the structural members and the finite element analysis) were higher than the load differences obtained when the hypotheses of no settlements and measured settlements have been compared, but the same structural model (the finite element model) was used. This has been attributed to the characteristics of the building and also to the small measured settlements used in the analysis.

• The strains in columns - aiming at the evaluation of the column loads - have been measured from the beginning of construction. The loads obtained from the strain values measured (*N*), taking into account the strains due to creep and shrinkage, have been compared with the loads obtained from the finite element analysis, considering the structure subjected to the measured settlements (*Nprog*). A good agreement between these loads is obtained only in the first stage of column C10. A trend of higher *N* values than *Nprog* values was obtained in the first stage while the opposite was found as time progresses. It is believed that the strain due to concrete shrinkage (or even the concrete creep) has been overestimated. There is an urgent need of measurements of strain in columns from the beginning of construction, as well as the improvement of the ability to predict the concrete strains due to creep and shrinkage in reinforced concrete columns of different shapes in order to properly evaluate the column loads in buildings.

Acknowledgements

The comments and suggestions made by Professor Nelson Aoki have been greatly appreciated. The Brazilian Research Council, CNPq, has provided a grant to the first author.

References

Aoki, N. (1997) Geotechnical aspects of soil-structure interaction. Proc. XXVIII South-American Conference on Structural Engineering, São Carlos, v. 1, p. 7-11 (in Portuguese).

Chamecki, S. (1954) The influence of the structural stiffness on the evaluation of foundations settlements. Proc.

I Brazilian Conference on Soil Mechanics and Foundation Engineering, Porto Alegre, v. 1, p. 35-80 (in Portuguese).

CEB-FIP Model Code (1990), Comite Euro-International du Beton. Design Code, Thomas Telford, p. 33-81.

Costa, R.V. (2003) Case Histories of the Measurement of Foundations Settlements From the Beginning of Construction. M.Sc. Thesis, UFF, Niterói, 147 pp. (in Portuguese).

Danziger, B.R.; Danziger, F.AB. & Crispel, F.A. (2000) The measurement of settlements from the beginning of construction as a foundation quality control. Proc. IV Seminar of Special Foundations and Geotechnics, SEFE IV, São Paulo, v. 1, p. 191-202 (in Portuguese).

Danziger, F.A.B.; Barata, F.E.; Santa Maria, P.E.L.; Danziger, B.R. & Crispel, F.A. (1997) Measurement of settlements and strains on buildings from the beginning of construction. Proc. XIV International Conference on Soil Mechanics and Foundation Engineering, Hamburg, v. 2, p. 787-788.

Danziger, F.A.B.; Santa Maria, P.E.L.; Gonçalves, A.V.S. & Crispel, F.A. (1995) Quality control of foundations: the measurement of settlements from the beginning of construction. Proc. Braz. Seminar on Technology of Buildings, ENTAC'95, Rio de Janeiro, v. 1, p. 125-130 (in Portuguese).

Gonçalves, J.C. (2004) The Influence of Settlements on the Columns Loads of a Building. M.Sc. Thesis, COPPE, Universidade Federal do Rio de Janeiro, Rio de Janeiro, 126 pp. (in Portuguese).

Gonçalves, J.C.; Danziger, F.A.B.; Santa Maria, P.E.L. & Crispel, F.A. (2004) Comparison between measured and predicted settlements of a building in shallow foundations. Proc. V Seminar of Special Foundations and Geotechnics, SEFE V, São Paulo, v. 2, p. 290-299 (in Portuguese).

Goschy, B. (1978) Soil-foundation-structure interaction. Journal of the Structural Division, v. 104:ST5, p. 749-761.

Gusmão, A.D. (1990) Soil-Structure Interaction and its Influence on the Settlements of Foundations. M.Sc. Thesis, COPPE, Universidade Federal do Rio de Janeiro, Rio de Janeiro, 165 pp. (in Portuguese).

Gusmão, A.D. & Gusmão Filho, J.A. (1994a) Soil-structure interaction in buildings. Proc. X Brazilian Conference on Soil Mechanics and Foundation Engineering, Salvador, v. 2, p. 447-454 (in Portuguese).

Gusmão, A.D. & Gusmão Filho, J.A. (1994b) Construction sequency effect on settlements of buildings. Proc XIII International Conference on Soil Mechanics and Foundation Engineering, New Delhi, v. 2, p. 1803-1806.

Gusmão Filho, J.A. (1998) Foundations: From Geology to Engineering Practice. Editora da Universidade Federal de Pernambuco, Pernambuco (in Portuguese).

Meyerhof, G.G. (1953) Some recent foundation research and its application to design. Structural Engineering, v. 31, p. 151-167.

Moura, A.R.L.U. (1995) Soil-Structure Interaction in Buildings. M.Sc. Thesis, Universidade Federal de Pernambuco, Pernambuco, 135 pp. (in Portuguese).

Russo Neto, L. (2005) Analysis of Strains and Settlements Measured During the Construction of a Concrete Structure with Driven Pile Foundations. D.Sc. Thesis, Escola de Engenharia de São Carlos, Universidade de São Paulo, São Carlos, 280 pp. (in Portuguese).

Santa Maria, F.C.M. (1997) Linear Viscoelasticity Applied to Problems of Consolidation and Soil-Structure Interaction. D.Sc. Qualifying Publication, COPPE, Universidade Federal do Rio de Janeiro, Rio de Janeiro, 154 pp. (in Portuguese).

Santa Maria, P.E.L.; Santa Maria, F.C.M. & Santos, A.B. (1999) Analysis of continuous beams resting on viscoelastic supports and its application to problems of soil-structure interaction. Soils & Rocks, v. 22:3, p. 179-194 (in Portuguese).

SAP 2000 (1996) SAP 2000 Analysis Reference v. 9.0. Computers and Structures Inc., California, USA, 430 p.

Soares, J.M. (2004) Numerical-Experimental Analysis of Soil-Structure Interaction of Two Buildings in Distrito Federal. D. Sc. Thesis, Universidade Federal de Brasília, Brasília (in Portuguese).

Soares, M.M. (1978) Preliminary analysis of the measurements carried out in an instrumented slurry wall built in Rio de Janeiro subway. Proc. 6th Brazilian Conference on Soil Mechanics and Foundation Engineering, Rio de Janeiro, v. II, p. 221-238 (in Portuguese).

Soares, M.M. & Carim, P.R.V. (1978) Some considerations on the precompression in struts used in slurry walls of the Rio de Janeiro subway. Proc. 6th Brazilian Conference on Soil Mechanics and Foundation Engineering, Rio de Janeiro, v. II, p. 239-251 (in Portuguese).

Case History

The Breach Problems in the Tunnels of the Boston Central Artery/Tunnel Project (Big Dig)

John T. Christian

Abstract. The Boston Central Artery/Tunnel (CAT) project consists of some 200 lane-kilometers of bridges, tunnels, and surface roadways. The central part of the project involves constructing two directions of multi-lane roadway to depths exceeding 30 m beneath the existing city by means of the slurry wall technique. The resulting walls, called Soldier Pile Tremmie Concrete (SPTC) walls, held back the *in situ* soils, supported an existing elevated roadway during construction, and form the final walls of the new tunnels. In September 2004 a breach occurred in one panel in the deepest section of the tunnel, spewing water onto the roadway and creating a crisis of public confidence in the project. Investigation revealed that the breach resulted from a series of shortcomings in construction and inspection, for which the relevant parties took responsibility. Three alternate repair schemes were proposed. Selecting the best procedure involved not only technical considerations but also impacts on neighboring high-rise buildings. The incident has implications for the construction of deep slurry walls in congested areas.

Key words: slurry walls, tunnels, construction, dewatering.

1. Introduction

The Boston Central Artery/Tunnel Project (CAT) is one of the largest civil engineering projects in history. The project consists essentially of three parts: (1) construction of an underwater vehicular tunnel under the harbor to connect the end of the Massachusetts Turnpike (Interstate Route I-90) to Logan Airport and other points in East Boston, (2) replacing the existing elevated vehicular expressway (Interstate Route I-93 – known as the “Central Artery”) with a system of underground tunnels, and (3) replacing a set of roads and bridges that connects the northern end of the Central Artery to other roads. Originally authorized in 1986 at US$ 2,6 billion and scheduled for completion in 1998, the project is now budgeted at US$ 14,625 billion with a completion date in 2006. Because of these escallations and public disputes over several of the proposed design schemes, the project has become the focus of wide-ranging and continuing controversy. In this context, the appearance in September 2004 of breaches with flowing water in a wall of the deepest section of the I-93 tunnel was the subject of intense scrutiny in the press and by regulatory agencies. How had the breach occurred, and how could it be repaired?

2. Project Configuration

The project takes place in an exceptionally crowded urban environment, with high rise buildings, critical operating plants, and railroad facilities located within meters of the proposed rights of way. Furthermore, it was necessary to keep the existing elevated expressway operating until the new road could be completed to a stage that could accommodate the high desity of traffic.

The solution adopted for the main I-93 tunnels was to install slurry walls along the new right of way with 0.91 m (36 in) H-piles placed in the slurry on approximately 1.52 m (5 ft) centers and bearing on the bedrock. A small protion of the walls incorporated reinforcing cages as well. In each panel concrete was trimmed in to replace the slurry, and, after all panels were completed, the resulting wall consisted of a thickness approximately 1.07 m (3.5 feet) of concrete

Figure 1 - Map of CAT Project.

John T. Christian, Consulting Engineer, Waban, Massachusetts, USA. e-mail: christian1@rcn.com.
Submitted on September 14, 2006; Final Acceptance on June 15, 2007; Discussion open until April 30, 2008.

with steel H-piles embedded along its length. The major structural loads were carried by approximately 9600 steel H-piles, and the concrete acted primarily in shear to transfer the loads of soil and water to the piles. These composite walls would become the final walls of the tunnels. The tunnels were constructed by a top-down procedure with cross-lot bracing installed as the excavation proceeded. Upon completion of the tunnel sections, the overlying region was backfilled. The walls are known in the terminology of the project as Soldier Pile Tremmis Concrete (SPTC) walls. Figure 2 shows a simplified cross section of the tunnel.

The existing elevated expressway had been supported by columns that in turn carried the loads to the bedrock. The construction procedure was to transfer the loads from the existing piles to the new H-piles in the slurry walls. Thus, once the tunnels had been completed, the traffic could be diverted into the new tunnels and the previously existing elevated structure demolished.

A further complication is that the elevation of the tunnels vary considerably over their lengths. As can be seen in Fig. 3, the I-93 tunnel comes from the south (the left of the figure), drops to its deepest point to pass under the existing red line metro line, rises nearly to the surface to pass over the blue metro line, drops down again to pass under the access ramps for the existing Sumner and Callahan tunnels across the harbor, and rises to connect to the new Zakim bridge across the Charles river. Thus, a considerable variety of loadings and soil conditions occurs even in this short distance. The section that is the principal subject of this paper is in the deepest part of the project just north of the red line.

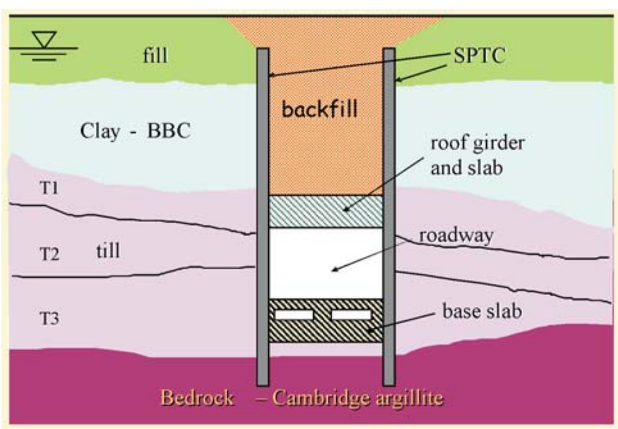

Figure 2 - Simplified cross-section of tunnel.

3. The Breach and its Cause

In September 2004, after the tunnel had been opened to traffic for nearly a year, a breach occurred in one of the tunnels walls. Water gushed onto the roadway, forcing the authorities to close the tunnel to traffic and to initiate emergency procedures to stanch the flow.

Investigation revealed that the breach had occurred at a point in the tunnel where the soil outside the tunnel is the T3 till (Fig. 2). Although all three of the tills are sense as a result of compaction under the weight of Pleaistocene glaciers, the T3 segment consists of sands and gravels with little or no silt and clay, so that the permeability of the soil is much higher than that of the other tills and the overlying clay. Since the water table is at or near the surface, the head of approximately 21.3 m (70 ft) can drive a substantial flow of water. The questions then was to discover how the breach in the concrete had come about.

Figure 4 illustrates the construction sequence for the soldier pile tremmie concrete (SPTC) walls. When the soldier piles are placed in the slurry, the space between the outside flanges is filled with an inert granualr material and the space closed off with an end stop, which is made of plywood or thin steel plate. When the secondary panel is excavated,. it is essential that the end stop and the granular material be removed so the concrete for the secondary panel makes good contact with the steel pile.

In the present case the contractor for one section of the tunnel poured too much concrete at the end of the last

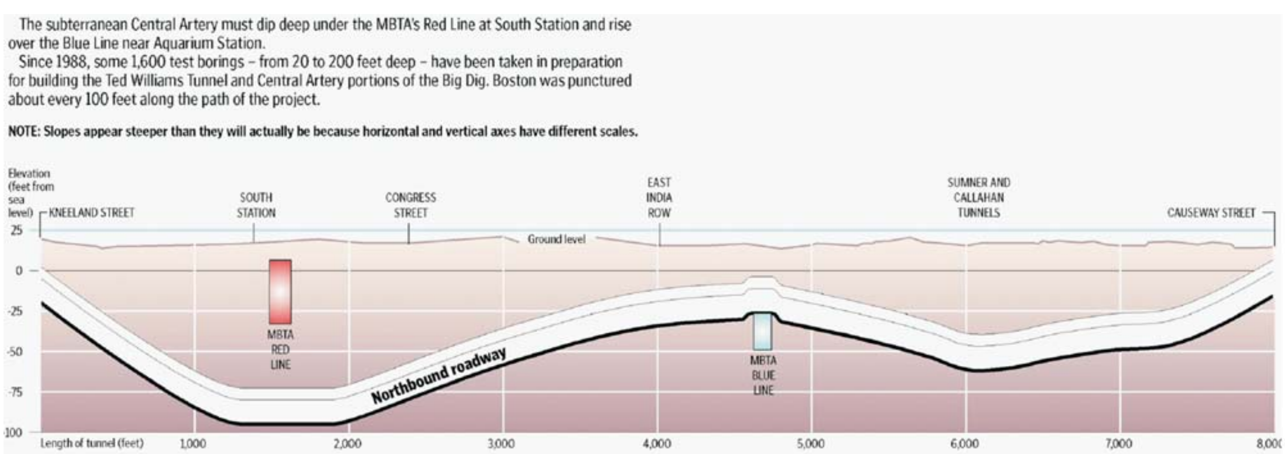

Figure 3 - Elevation along length of I-93 tunnel.

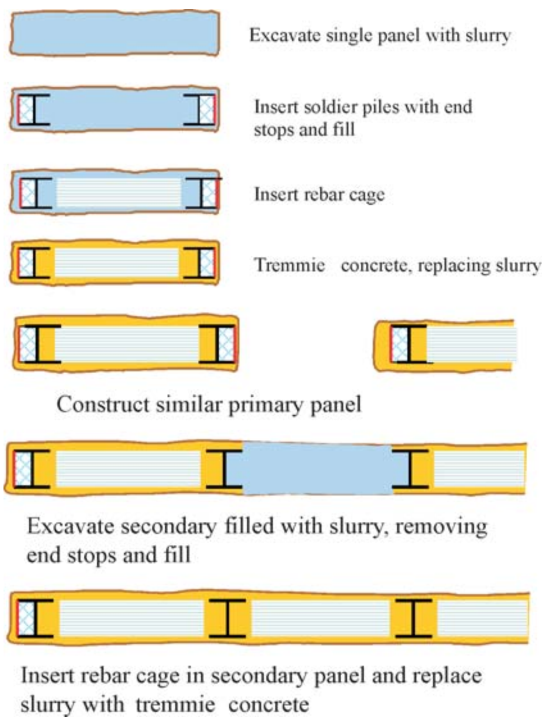

Figure 4 - Construction sequence for SPTC wall.

primary panel, creating a mass of concrete that intruded into what would become a secondary panel placed by the contractor for the next section. Rather than excavating the block of extra concrete, that contractor simply tried to excavate under it. This was not successful, so a portion of the soil lying under the excess mass was never excavated and was incorporated in the final wall. Part of this material was T3 till, through which the flow eventually occurred.

The configuration of the leak is depicted in Fig. 5, which shows an elevation as seen from the inside of the tunnel and a horizontal section through the breach. This was clearly the result of faulty construction and inadequate inspection; both the engineers and the contractor accepted responsibility for repairing the wall. Unfortunately, all this had to be done in a highly politicized environment with constant attention from the press.

4. Repair Alternatives

Three alternatives presented themselves for repairing the wall. The first was to construct a new slurry wall panel outside of the damaged panel. This was rejected because no one could devise a method of creating a water-tight connection to the rest of the wall and because it would be necessary to place construction machinery on a busy street and in the entrance to the Federal Reserve Bank.

The second proposed solution was to excavate all of the damage section of the wall and replace it with a reinforced concrete panel. This would have required building the new wall section in horizontal lifts over several weeks since the continued operation of the tunnel meant that work had to be done in four hour windows in the early morning hours. A more serious problem with this solution was that it required dewatering the work area by lowering the water table by approximately 70 ft. In addition to the difficulty of the dewatering itself, this raised the prospect of settlement damage to neighboring structures and the hazards associated with the possible failure of the pumping system during the protracted construction. During the construction the stability of the wall would depend entirely on the continued operation of the pumping system. At least one prominent consultant to the project argued forcefully for this solution, but the consensus of the other engineers was to use the final alternative.

The third alternative, which was adopted, was to keep the damaged section in place and to place a reinforced plate in front of it to contain the water forces. Figure 6 illustrates the details. The plate consisted of a steel plate stiffened by 0.20 m (8 in) steel beams and encased in concrete. The panel was designed to carry all the loads for which the origianl panel was designed, so that any capacity in the damaged section provided an additional margin of safety. The replacement panel was designed by one structural engineering firm and the design checked by two others. The project engineers concluded that this solution represents a conservative, robust solution. The panel has been installed, and is functioning well.

5. Conclusions

Aside from the issues addressed during the design for this particular problem, some more general conclusions can be drawn. Among them are:

(a) Installing slurry walls at depth is difficult. It is hard to control the excavation and construction processes at depths greater than about 20 m (65 ft). Engineers contemplating installing walls below this depth should consider carefully how the wall will be designed and built and how the performance of the wall will be assured.

(b) Both construction and inpection of deep walls shuld meet the highest standards.

(c) If the wall is to serve as the final wall and snot simply an interim construction measure, the wall should be power washed before acceptance. In the present case the materials in the wall section were concrete, some slurry, and the unexcavated till. All of these are grey, and, in the dim light in the tunnel excavation, it is not easy to tell them apart without washing the wall vigorously.

Acknowledgements

This work was done by a large number of engineers at the Massachusetts Turnpike Authority, the CA/T Project, and various consulting firms. Michael P. Lewis is the Project Director for the CA/T Project; he gave the author permission to present this material.

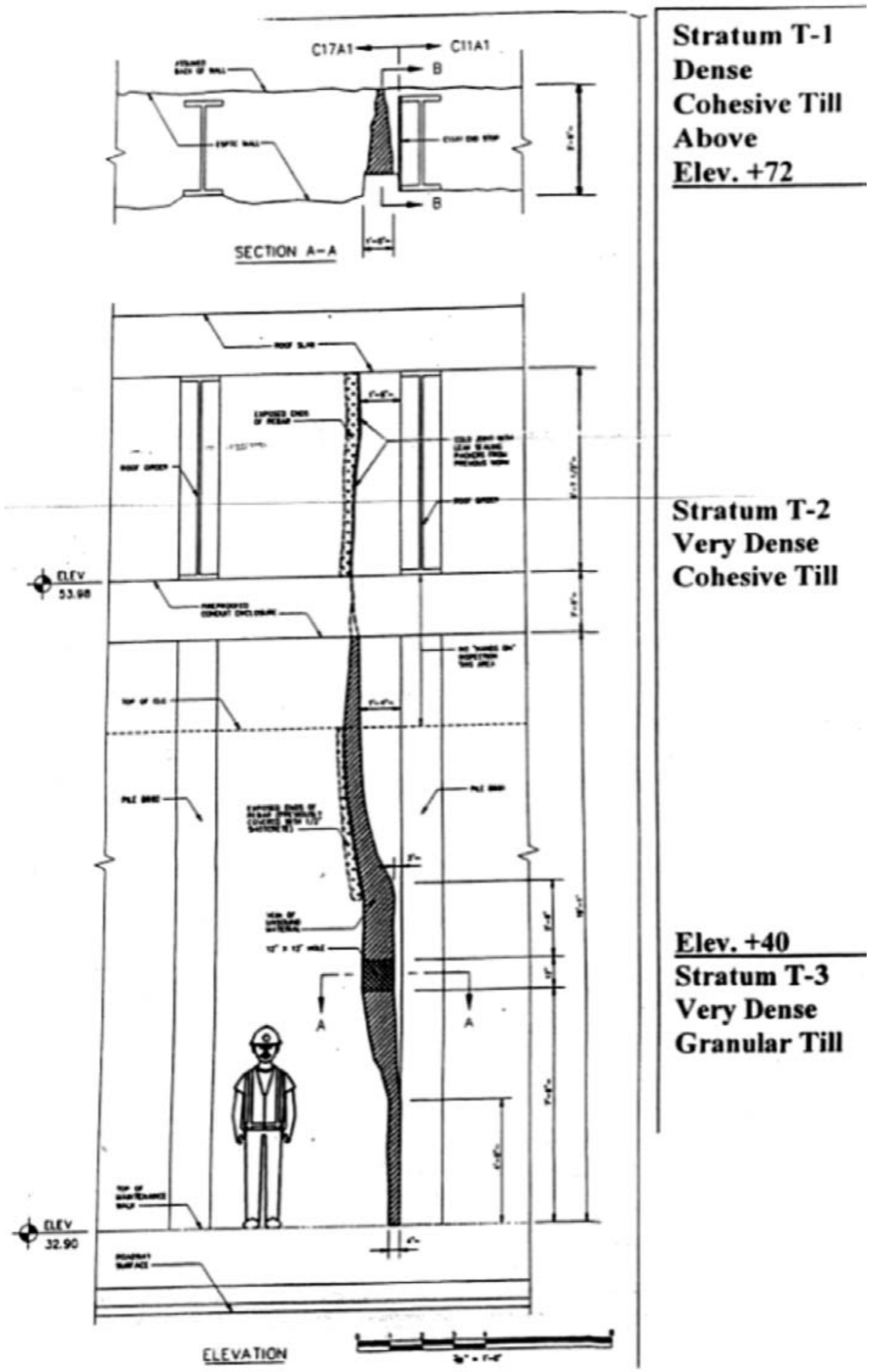

Figure 5 - The breach in the SPTC wall.

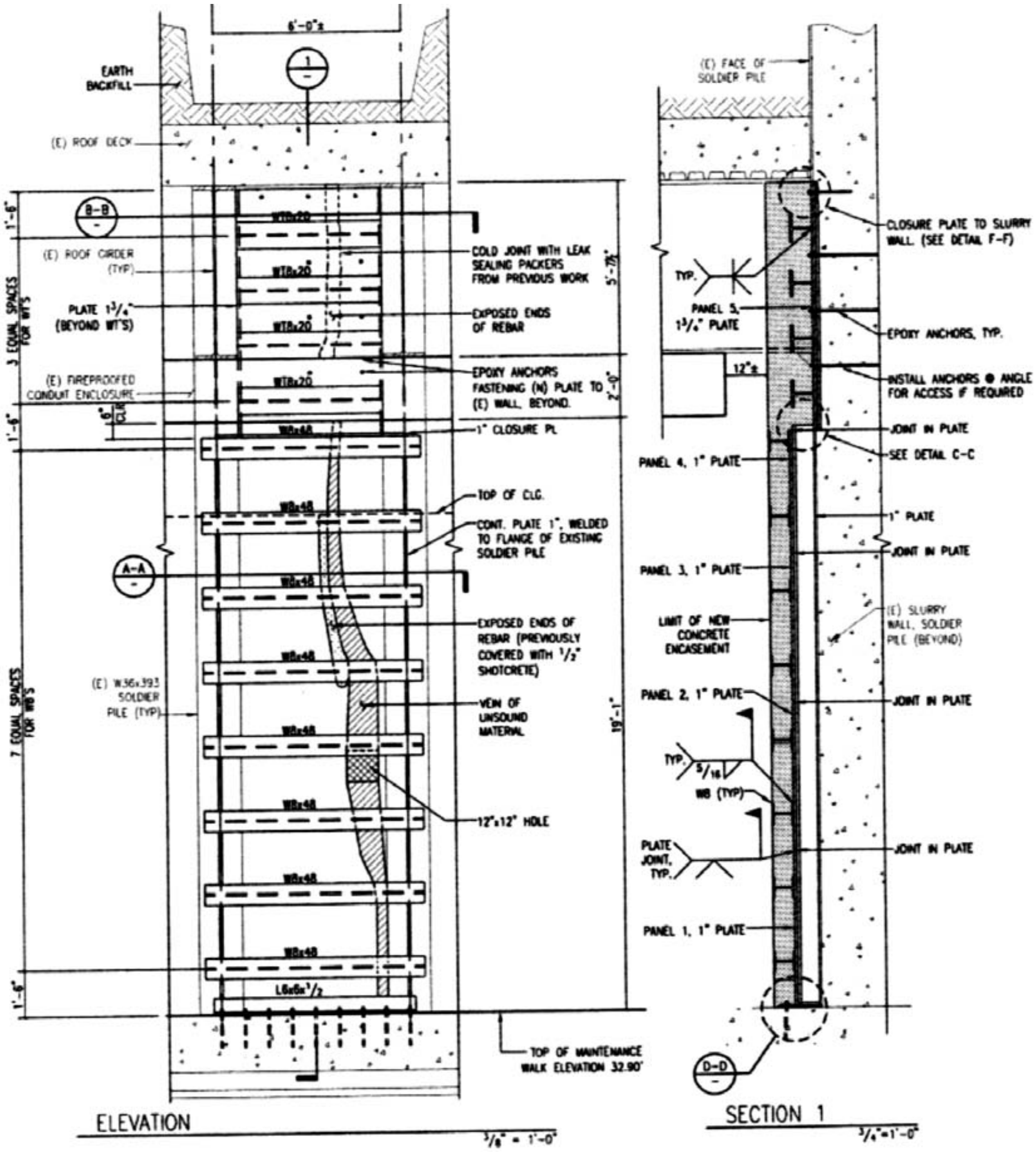

Figure 6 - The solution adopted.

SOILS and ROCKS
An International Journal of Geotechnical and Geoenvironmental

Publication of
ABMS - Brazilian Association for Soil Mechanics and Geotechnical Engineering
ABGE - Brazilian Association for Engineering Geology and the Environment
SPG - Portuguese Geotechnical Society

Volume 30, N. 3, September-December 2007

Author index

Instructions to Authors

Category of the Papers

Soils and Rocks is the scientific journal edited by the Brazilian Society of Soil Mechanics and Geotechnical Engineering (ABMS) and by the Brazilian Society of Engineering and Environmental Geology (ABGE). The journal is intended to the divulgation of original research works from all geotechnical branches.

The accepted papers are classified either as an Article paper, a Technical Note, a Case Study, or a Discussion according to its content. An article paper is an extensive and conclusive dissertation about a geotechnical topic. A paper is considered as a technical note if it gives a short description of ongoing studies, comprising partial results and/or particular aspects of the investigation. A case study is a report of unusual problems found during the design, construction or the performance of geotechnical projects. A case study is also considered as the report of an unusual solution given to an ordinary problem. The discussions about published papers, case studies and technical notes are made in the Discussions Section.

When submitting a manuscript for review, the authors should indicate the category of the manuscript, and is also understood that they:

a) assume full responsibility for the contents and accuracy of the information in the paper;

b) assure that the paper has not been previously published, and is not being submitted to any other periodical for publication.

Manuscript Instructions

Manuscripts must be written in English. The text is to be typed in a word processor (MS Word or equivalent), using ISO A4 page size, left, right, top, and bottom margins of 25 mm, Times New Roman 12 font, and line spacing of 1.5. All lines and pages should be numbered. The text should be written in the third person.

The fist page of the manuscript is to include the title of the paper in English, followed by the names of the authors with the abbreviation of the most relevant academic title. The affiliation, address and e-mail is to be indicated below each author's name. An abstract of 200 words is to be written in the language of the paper after the author's names. Translations of the abstract in the other languages are to follow the abstract. A list with up to six keywords at the end of the abstract and each translation is required.

Although alteration of the sequence and the title of each section may be required, it is suggested that the text contains the following sections: Introduction, Material and Methods, Results, Discussions, Conclusion, Acknowledgements, References and List of Symbols. A brief description of each section is given next.

Introduction: This section should indicate the state of the art of the problem under evaluation, a description of the problem and the methods undertaken. The objective of the work is to be clearly presented at the end of the section.

Materials and Methods: This section should include all information needed to the reproduction of the presented work by other researchers.

Results: In this section the data of the investigation should be presented in a clear and concise way. Figures and tables should not repeat the same information.

Discussion: The analyses of the results should be described in this section. **Conclusions**: The text of this section should be based on the presented data and in the discussions.

Acknowledgenments: If necessary, concise acknowledgements should be written in this section.

References: References to other published sources are to be made in the text by the last name(s) of the author(s), followed by the year of publication, similarly to one of the two possibilities below:

"*while Silva & Pereira (1987) observed that resistance depended on soil density*" or "*It was observed that resistance depended on soil density (Silva & Pereira, 1987).*"

In the case of three or more authors, the reduced format must be used, *e.g.*: Silva *et al.* (1982) or (Silva *et al.*, 1982). Two or more citations belonging to the same author(s) and published in the same year are to be distinguished with small letters, *e.g.*: (Silva, 1975a, b, c.). Standards must be cited in the text by the initials of the entity and the year of publication, *e.g.*: ABNT (1996), ASTM (2003).

Full references shall be listed alphabetically at the end of the text by the first author's last name. Several references belonging to the same author shall be cited chronologically. Some examples are listed next:

Papers: Bishop, A.W. & Blight, G.E. (1963) Some aspects of effective stress in saturated and unsaturated soils. Géotechnique, v. 13:2, p. 177-197.

Books: Lambe, T.W & Whitman, R.V. (1979) Soil Mechanics, SI Version, 2nd ed. John Wiley & Sons, New York, p. 553.

Book with editors: Sharma, H.D.; Dukes, M.T. & Olsen, D.M. (1990) Field measurements of dynamic moduli and Poisson's ratios of refuse and underlying soils at a landfill site. Landva A. & Knowles, G.D. (eds) Geotechnics of Waste Fills - Theory and Practice, American Society for Testing and Materials - STP 1070, Philadelphia, p. 57-70.

Proceedings (printed matter or CD-ROM): Jamiolkowski, M.; Ladd, C.C.; Germaine, J.T & Lancellotta, R. (1985) New developments in field and laboratory testing of soils. Proc. 11th Int. Conf. on Soil Mech. and Found. Engn., ISSMFE, San Francisco, v. 1, pp. 57-153.(specify if CD – ROM)

Thesis and dissertations: Lee, K.L. (1965) Triaxial Compressive Strength of Saturated Sands Under Seismic Loading Conditions. PhD Dissertation, Department of Civil Engineering, University of California, Berkeley, 521 p.

Standards: ASTM (2003) Standard Test Method for Particle Size Analysis of Soils - D 422-63. ASTM International, West Conshohocken, Pennsylvania, USA, 8 p.

Internet references: Soils and Rocks available at http://www.abms.com.br.

On line first publications must also bring the digital object identifier (DOI) at the end.

Figures shall be either computer generated or drawn with India ink on tracing paper. Computer generated figures must be accompanied by the corresponding digital file (.tif, .jpg, .pcx, etc.). All figures (graphs, line drawings, photographs, etc.) shall be numbered consecutively and have a caption consisting of the figure number and a brief title or description of the figure. This number should be used when referring to the figure in text. Photographs should be black and white, sharp, high contrasted and printed on glossy paper.

Tables shall be numbered consecutively in Arabic and have a caption consisting of the table number and a brief title. This number should be used when referring to the table in text. Units should be indicated in the first line of the table, below the title of each column. Abbreviations should be avoided. Column headings should not be abbreviated. When applicable, the units should come right below the corresponding column heading. Any necessary explanation can be placed as footnotes.

Equations shall appear isolated in a single line of the text. Numbers identifying equations must be flush with the right margin. International

System (SI) units are to be used. The symbols used in the equations shall be listed in the List of Symbols. It is recommended that the used symbols be in accordance with Lexicon in 8 Languages, ISSMFE (1981) and the ISRM List of Symbols.

The text of the submitted manuscript (including figures, tables and references) intended to be published as an article paper or a case history should not contain more than 30 pages formatted according to the instructions mentioned above. Technical notes and discussions should have no more than 15 and 8 pages, respectively. Longer manuscripts may be exceptionally accepted if the authors provide proper explanation for the need of the required extra space in the cover letter.

Discussion

Discussions must be written in English. The first page of a discussion paper should contain:

• The title of the paper under discussion in the language chosen for publication;

• Name of the author(s) of the discussion, followed by the position, affiliation, address and e-mail. The discusser(s) should refer himself (herself, themselves) as "the discusser(s)" and to the author(s) of the paper as "the author(s)".

Figures, tables and equations should be numbered following the same sequence of the original paper. All instructions previously mentioned for the preparation of article papers, case studies and technical notes also apply to the preparation of discussions.

Editorial Review

Each paper will be evaluated by reviewers selected by the editors according to the subject of the paper. The authors will be informed about the results of the review process. If the paper is accepted, the authors will be required to submit a version of the revised manuscript with the suggested modifications. If the manuscript is refused for publication, the authors will be informed about the reasons for rejection. In any situation comprising modification of the original text, classification of the manuscript in a category different from that proposed by the authors, or refusal for publication, the authors can reply presenting their reasons for disagreeing with the reviewers' comments

Submission

The author(s) must submit for review:

1. A hard copy of the manuscript to Editors - Soils and Rocks, Av. Prof. Almeida Prado, 532 – IPT, Prédio 54 – DEC/ABMS, 05508-901 - São Paulo, SP, Brazil. The first page of the manuscript should contain the identification of the author(s), or

2. The digital file of the manuscript, omitting the authors' name and any information that eventually could identify them, should be sent to **abms@ipt.br**. The following must be written in the subject of the e-mail message: "*Paper submitted to Soils and Rocks*". The authors' names, academic degrees and affiliations should be mentioned in the e-mail message. The e-mail address from which the digital file of the paper was sent will be the only one used by the editors for communication with the corresponding author.

Follow Up

The ABMS Secretariat will provide a password to the corresponding author, which will enable him/her to follow the reviewing process of the submitted manuscript at the ABMS website, clicking in the item menu "Fluxo de Trabalhos."

Volume 30, N. 3, September-December 2007

Table of Contents